Higgs Potential 2024
December 19 - 23, 2024,
University of Science and Technology of China (Hefei)

Higgs cross section measurements in the four-lepton final state using 2022 data at CMS

Tahir Javaid
(Beihang University, Beijing)

On behalf of the **CMS collaboration**

Outline

✳ **Overview**

✳ **Higgs differential cross section measurement**

- Strategy
- Results

✳ **Summary**

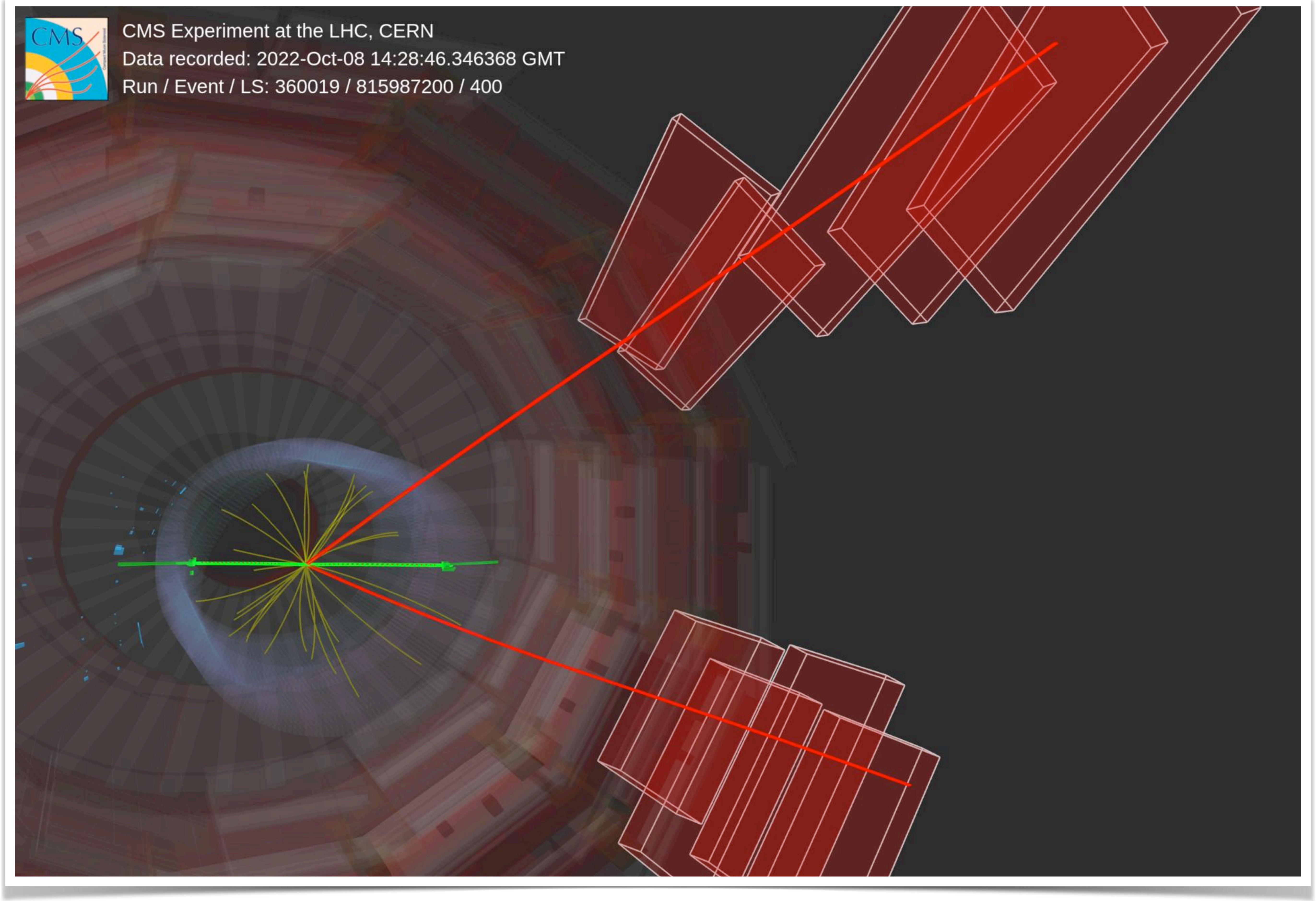

Overview

✳Higgs boson discovered in 2012 at CERN **(LHC Run1)**

✳LHC **Run2 and Run3** being eras of precision measurements

✳Its properties have been measured with evolving precision since the discovery

- Couplings, **cross-section** and etc.

✳Several decay modes studied so far.

https://doi.org/10.1038/s41586-022-04892-x

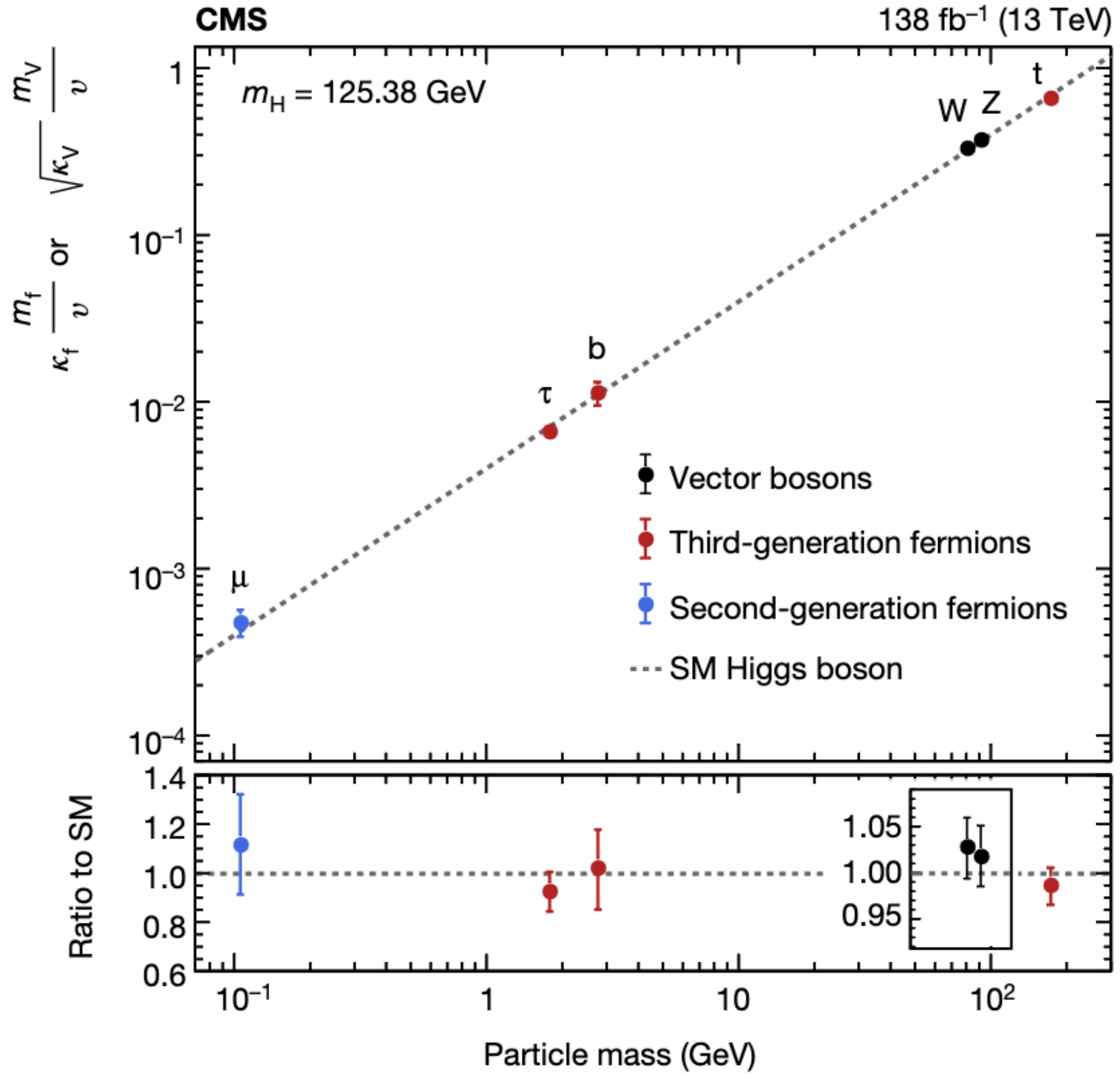

Recent results from CMS

Decay Channel	CMS data	Results	URL
H → ZZ → 4ℓ	Full Run2	Inclusive, differential (1D, 2D)	JHEP 08 (2023) 040
	Early Run3 (2022)	Inclusive, diffferential (1D)	CMS-PAS-HIG-24-013

Backup

This report

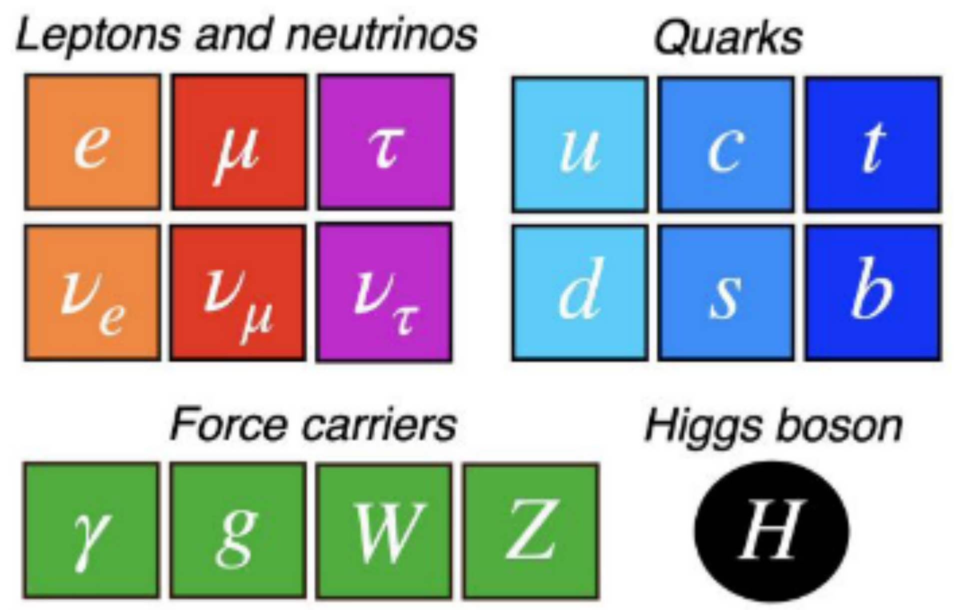

Overview: Higgs Production at LHC

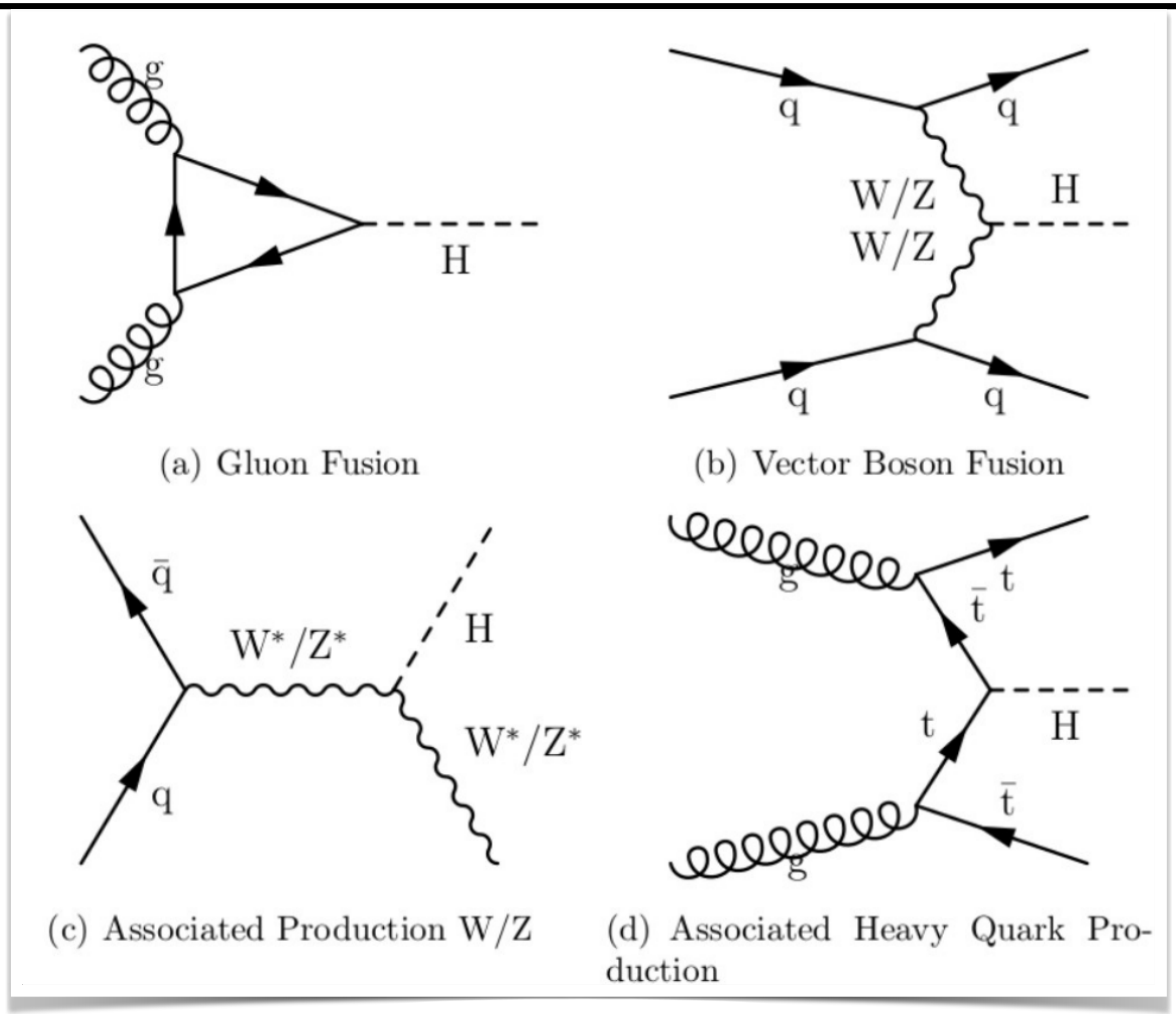

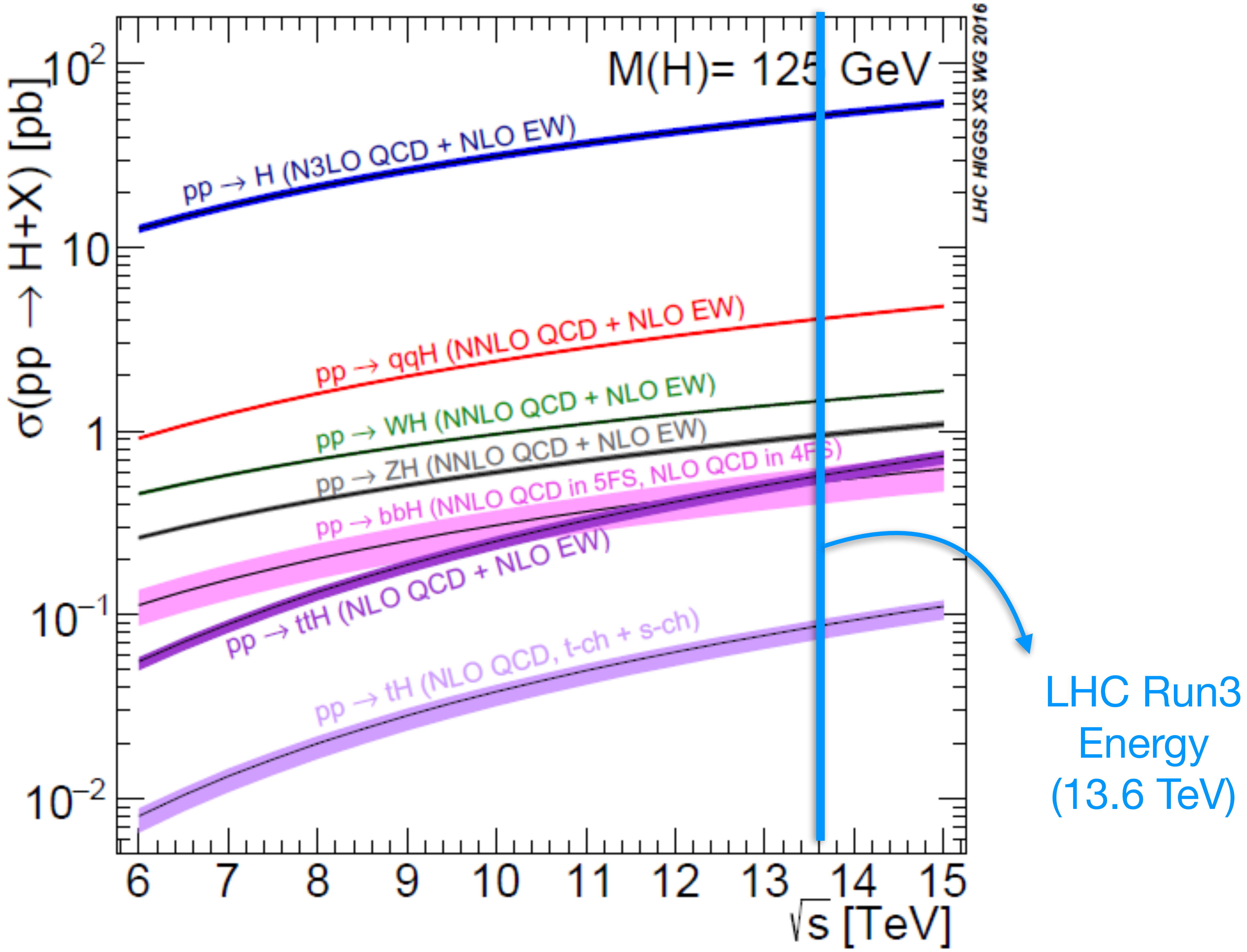

✳Significant increase in production cross sections from 8 TeV (Run1 2012) to 13.6 TeV (Run3)

- $\frac{\sigma_{13.6\ TeV}}{\sigma_{8\ TeV}}$ of:
  - Higgs production $\approx 2.95\ (ggH)$, $\approx 2.27\ (VBF)$, $\approx 1.92\ (VH)$ and $\approx 3.92\ (ttH)$
  - Background $\approx 2.35\ (Irreducible)$ and $\sim 2.5\ (Reducible)$

Overview: $H \to ZZ^* \to 4\ell$ decay mode and its motivation

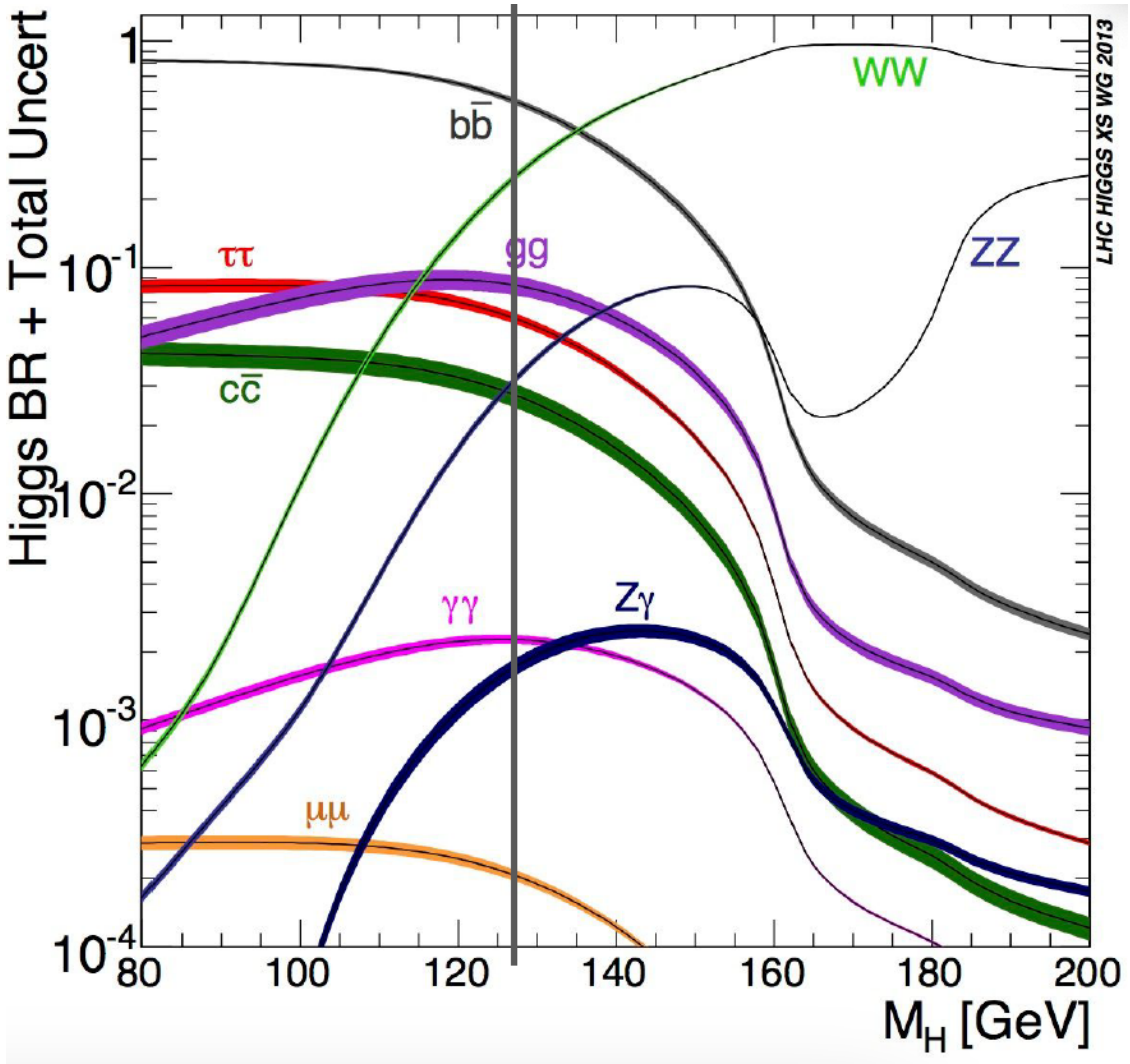

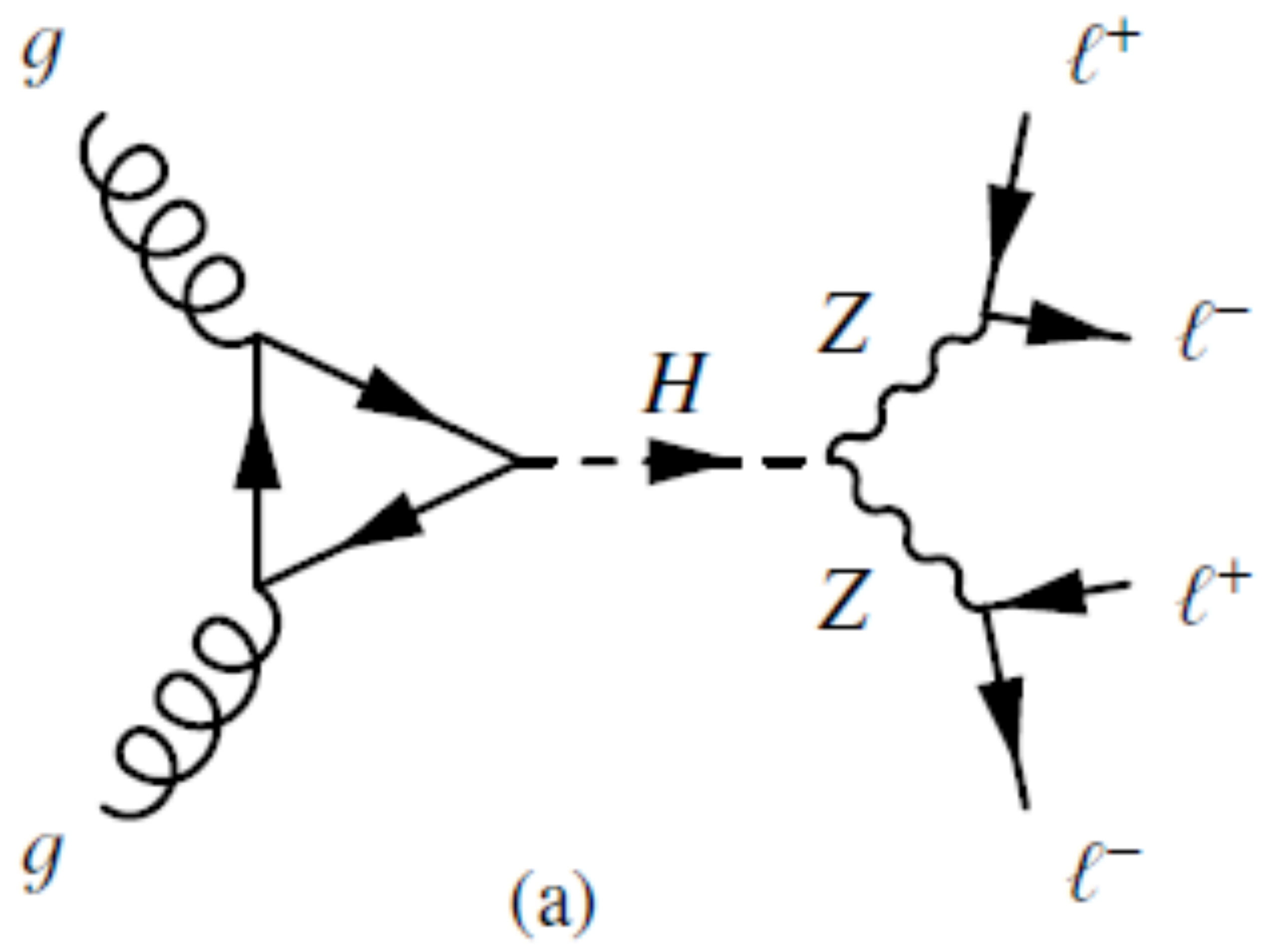

✳$\sigma \times Br\,(H \to ZZ^* \to 4\ell)$ is quite small

- Needs highest selection efficiency possible
- Efficient lepton identification over a broad p_T range

✳Event Signature:

- 4 leptons $(4e,\ 4\mu,\ 2e2\mu)$
- Large $\frac{S}{B}$ ratio $(> 2:1)$
- Good mass resolution $(\sim 1-2\%)$
- Four isolated leptons from one point in $3D$ space

✳Benefits from excellent electron and muon energy resolution

Object Selection: Electrons

✴Kinematic cuts

- $p_T > 7\ GeV$ and $|\eta| < 2.5$

✴Vertex cuts

- $d_{xy} < 0.5\ cm,\ d_Z < 1\ cm,\ |SIP_{3D}| < 4$

✴Identified and isolated by means of XGBoost classifier algorithm

- a switch from particle based isolations to cluster based isolations

	Cut on BDT score	Signal eff.	Background eff.
	$\lvert\eta\rvert < 0.8$		
	Cut on BDT score	Signal eff.	Background eff.
$5 < p_T < 10$ GeV	1.6339	81.64%	4.2%
$p_T > 10$ GeV	0.3685	97.45%	2.27%
	$0.8 < \lvert\eta\rvert < 1.479$		
	Cut on BDT score	Signal eff.	Background eff.
$5 < p_T < 10$ GeV	1.5499	80.31%	4.11%
$p_T > 10$ GeV	0.2662	96.68%	2.83%
	$\lvert\eta\rvert > 1.479$		
	Cut on BDT score	Signal eff.	Background eff.
$5 < p_T < 10$ GeV	2.0629	74.37%	2.97%
$p_T > 10$ GeV	-0.5444	96.62%	7.46%

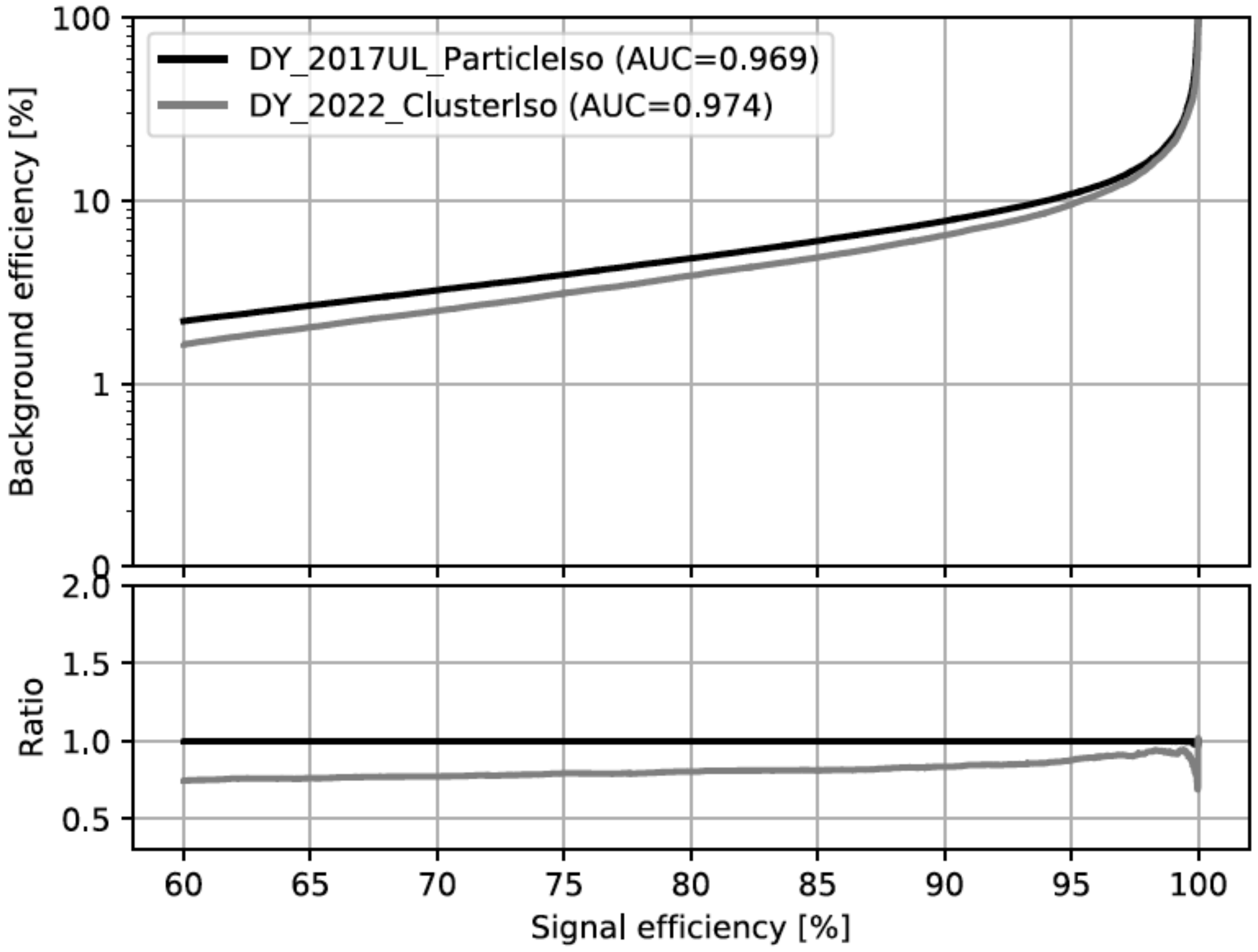

Object Selection: Electrons efficiency measurement (Tag and Probe Method)

✴Kinematic cuts

- $p_T > 7\ GeV$ and $|\eta| < 2.5$

✴Vertex cuts

- $d_{xy} < 0.5\ cm,\ d_Z < 1\ cm,\ |SIP_{3D}| < 4$

✴Identified and isolated by means of XGBoost classifier algorithm

- a switch from particle based isolations to cluster based isolations

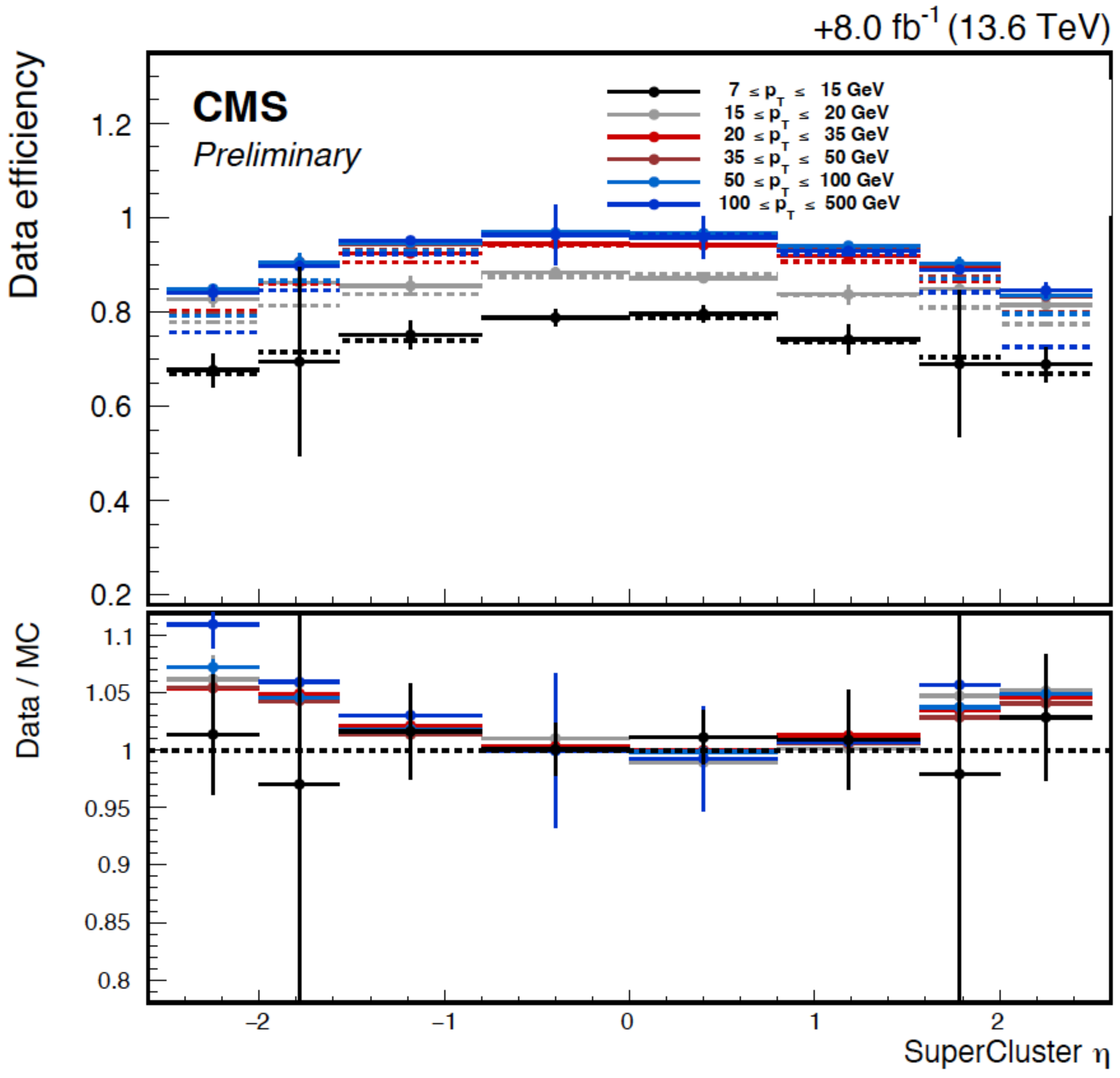

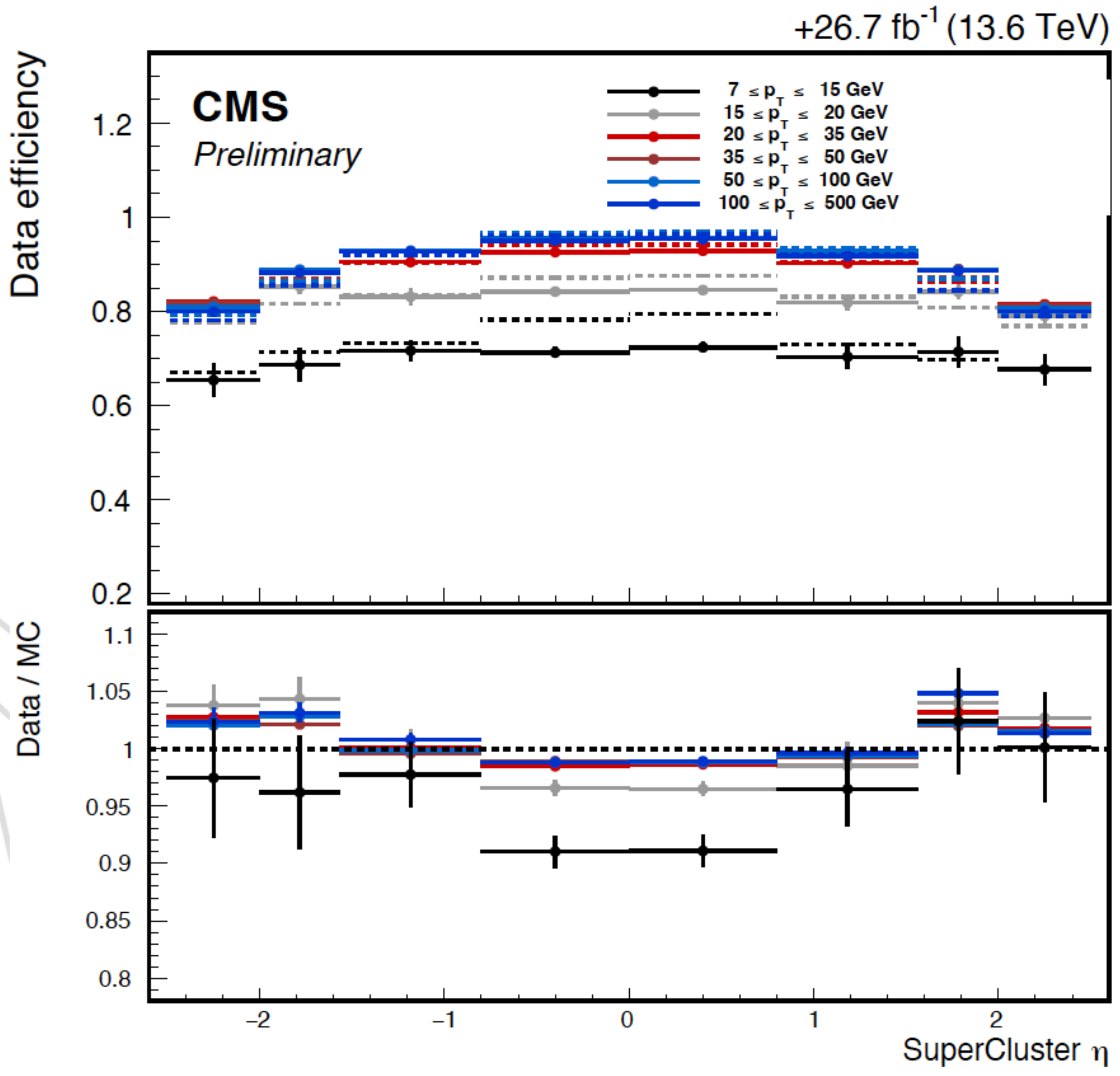

$$\epsilon = \epsilon_{reco.} * \epsilon_{sel.\ |\ reco.}$$

Object Selection: Muons

✴Kinematic cuts

- $p_T > 5\ GeV$ and $|\eta| < 2.5$

✴Vertex cuts

- $d_{xy} < 0.5\ cm,\ d_Z < 1\ cm,\ |SIP_{3D}| < 4$

✴Loose muons

- PF muon ID and tracker high p_T ID

✴Isolation

- $\mathcal{I}^{\mu}_{\mathrm{PF}}\ (\Delta R = 0.3) < 0.35$
- Isolation is $\Delta\beta$ PU corrected and applied after FSR recovery
  - *"Ghost-cleaning"* step performed

Object Selection: Muons efficiency measurement (Tag and Probe Method)

✴Kinematic cuts

- $p_T > 5\ GeV$ and $|\eta| < 2.5$

✴Vertex cuts

- $d_{xy} < 0.5\ cm,\ d_Z < 1\ cm,\ |SIP_{3D}| < 4$

✴Loose muons

- PF muon ID and tracker high p_T ID

✴Isolation

- $\mathcal{I}^{\mu}_{\mathrm{PF}}\ (\Delta R = 0.3) < 0.35$

$\epsilon_{total} = \epsilon_{Identification} * \epsilon_{IP} * \epsilon_{isolation}$

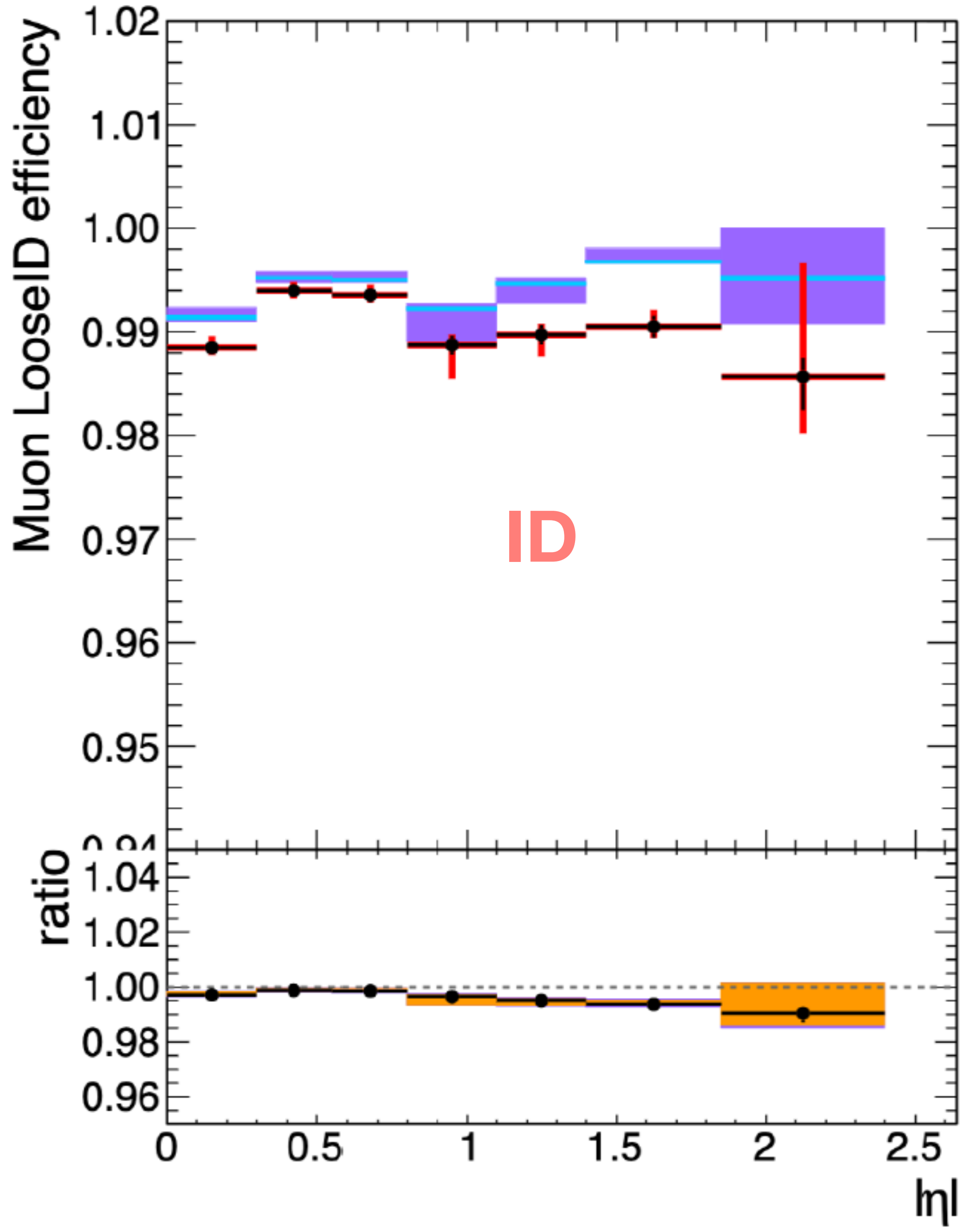

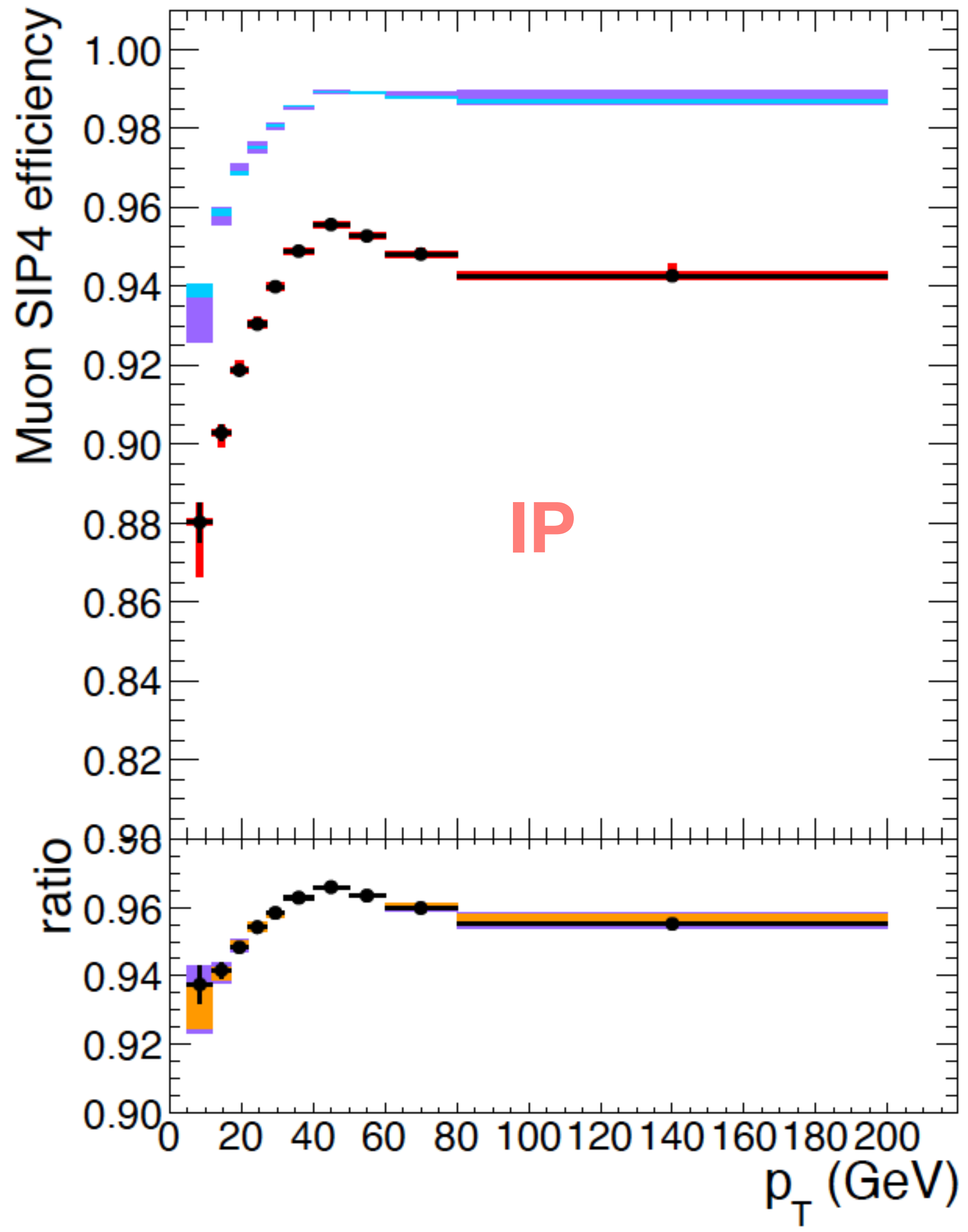

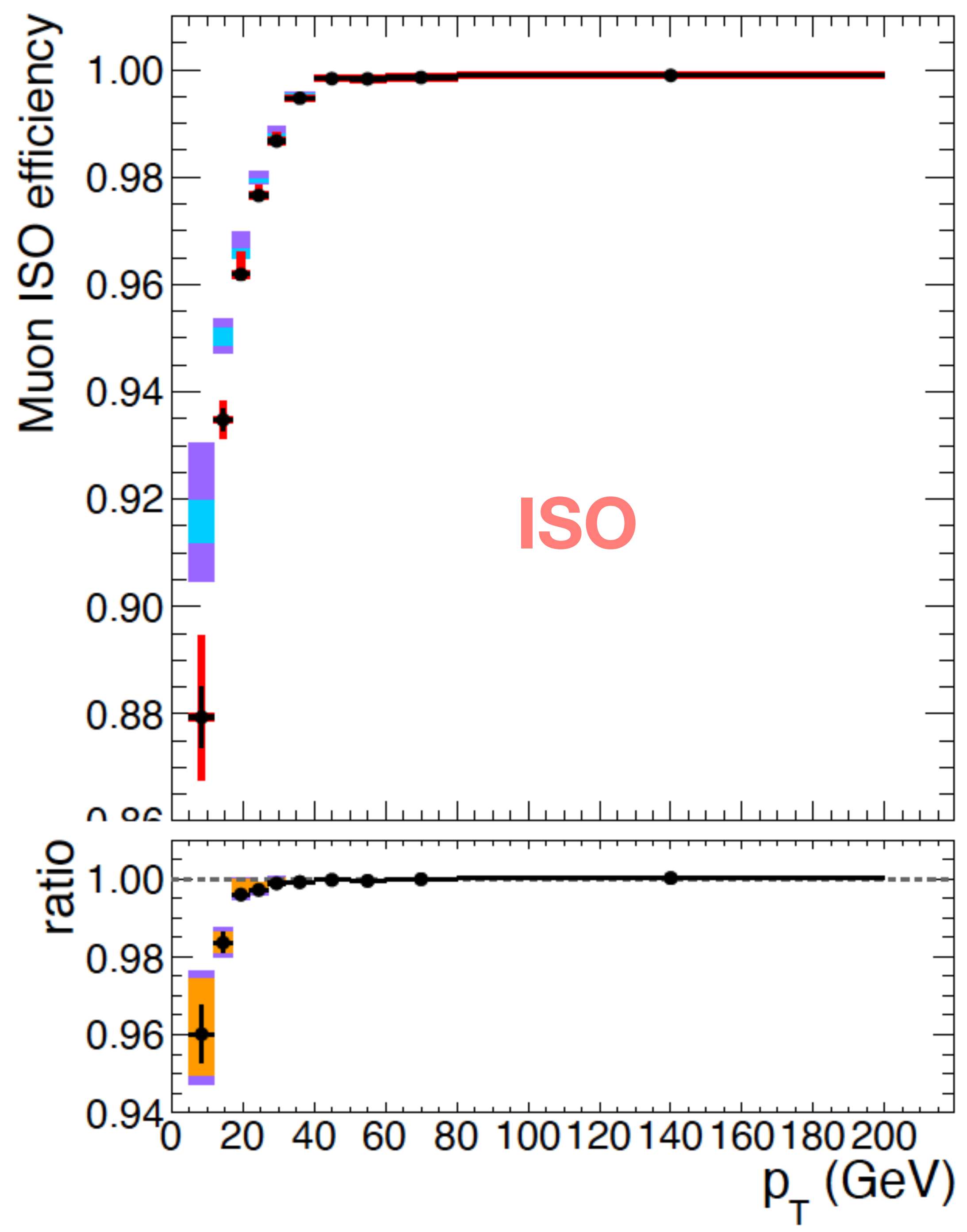

Background estimation

✳Irreducible Background

- Production of ZZ via qq annihilation or gluon fusion
- Estimated using *simulation*

✳Reducible Background

- Secondary leptons produced by heavy flavor jets
- $Z + jets,\ tt + jets,\ WZ,\ Z\gamma *, \ldots$
- Misidentified leptons coming from decays of heavy flavor hadrons, in-flight decays of light mesons within jets, or (for electrons) the decay of charged hadrons overlapping with π^0 decays
- Estimated using *data*
    - Fake Factor method

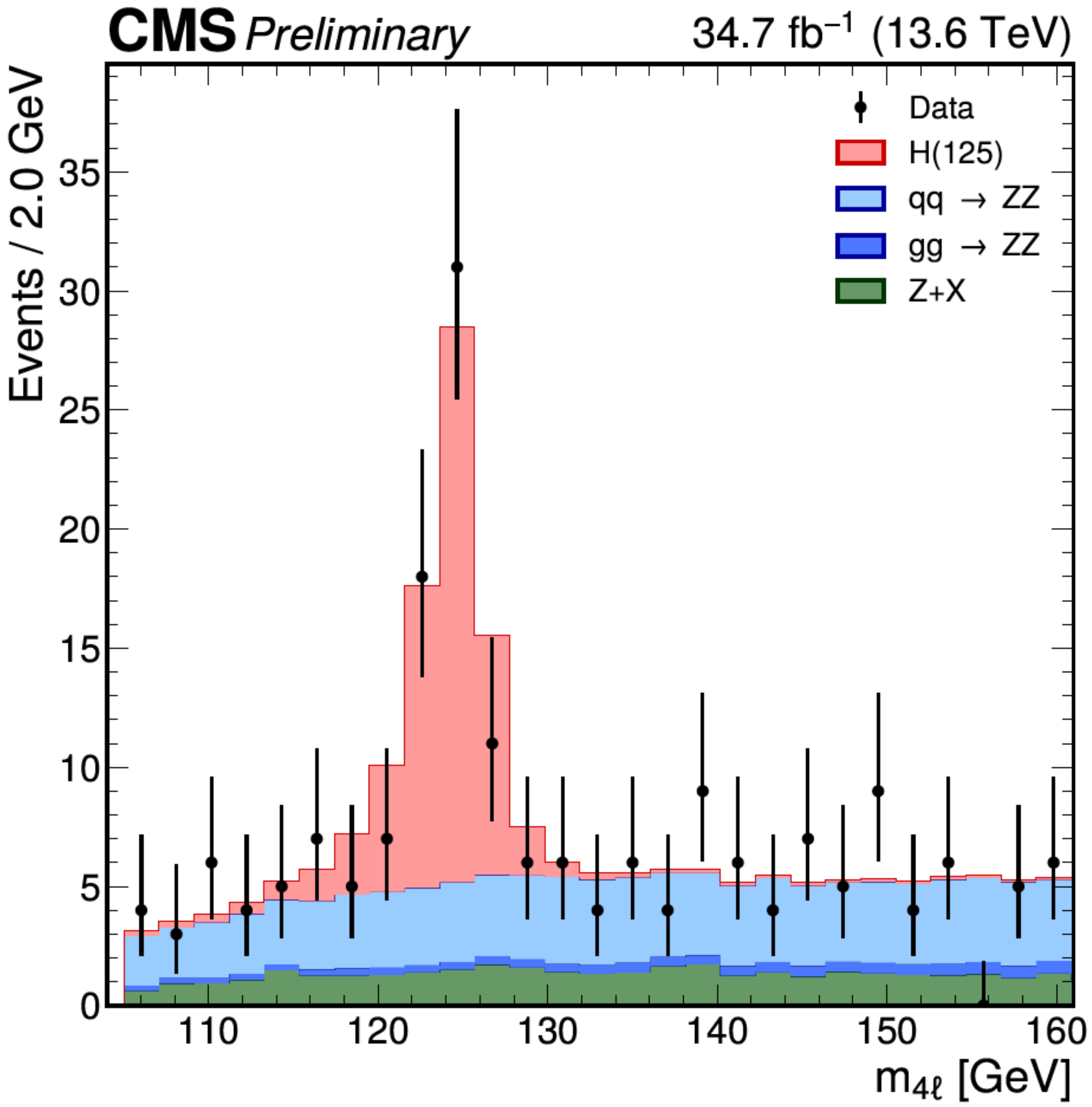

Analysis strategy: Cross section measurements in fiducial phase space

✳Necessary as cceptance has a strong model dependence

- Between SM production modes by up to 60%

✳Fiducial measurements have a key role

- Higgs cross sections can be measured in model independent way
- the extrapolation of the result is limited to a restricted phase space defined close as possible to the experimental selection
  - Minimizes the theoretical assumption for extrapolation to full phase space
  - Easy comparison with different theories

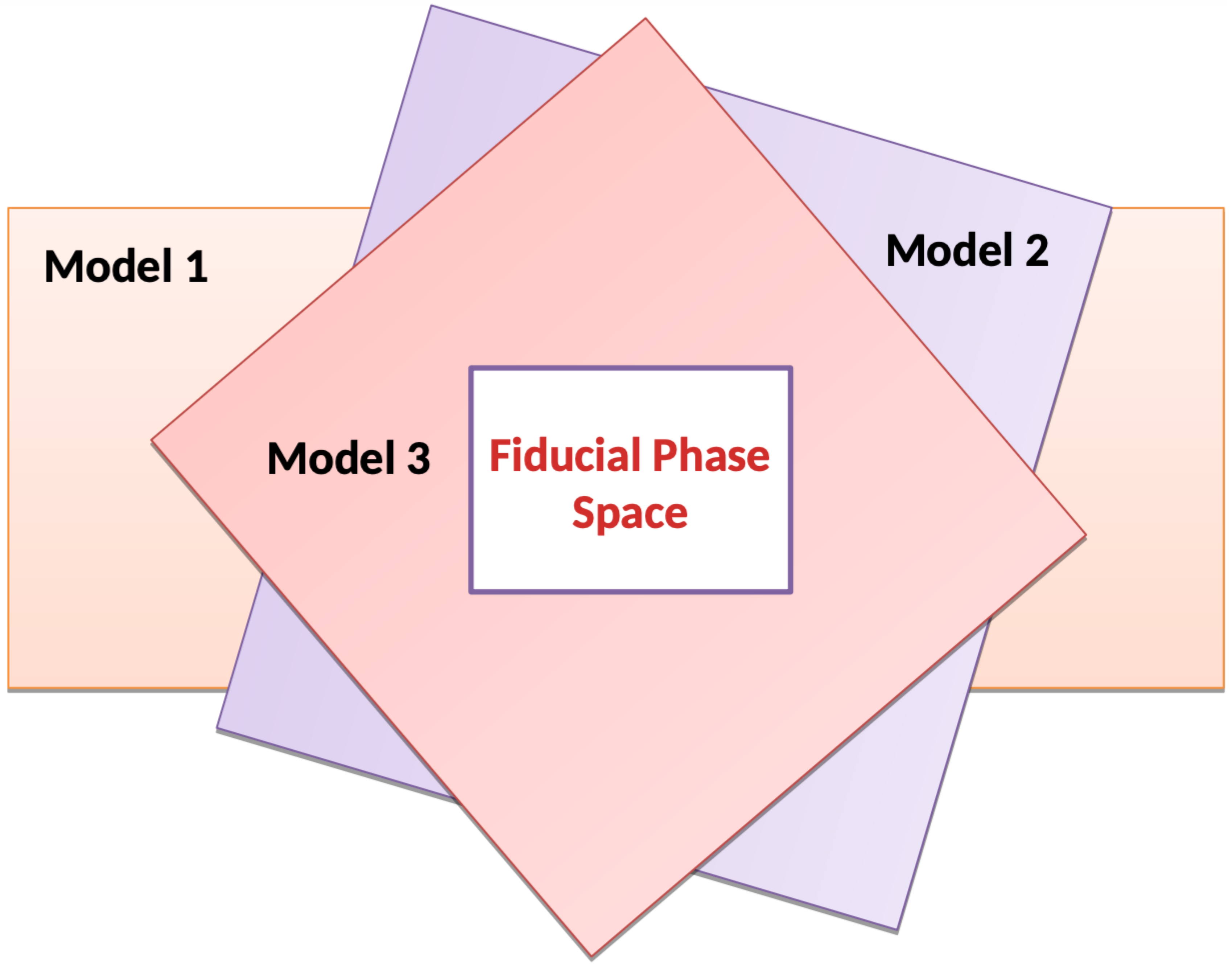

Signal process	$\mathcal{A}_{\text{fid}}$	ϵ	f_{nonfid}
Individual H boson production modes			
ggH	0.408 ± 0.001	0.625 ± 0.001	0.059 ± 0.001
VBF	0.456 ± 0.001	0.645 ± 0.002	0.043 ± 0.001
WH	0.353 ± 0.001	0.604 ± 0.001	0.113 ± 0.001
ZH	0.346 ± 0.001	0.620 ± 0.001	0.136 ± 0.001
$t\bar{t}H$	0.355 ± 0.001	0.603 ± 0.002	0.252 ± 0.002

Analysis strategy: Cross section measurements in fiducial phase space

✳Necessary as cceptance has a strong model dependence

- Between SM production modes by up to 60%

✳Fiducial measurements have a key role

- Higgs cross sections can be measured in model independent way
- the extrapolation of the result is limited to a restricted phase space defined close as possible to the experimental selection
  - Minimizes the theoretical assumption for extrapolation to full phase space
  - Easy comparison with different theories

Requirements for the H $\rightarrow 4\ell$ fiducial phase space	
Lepton kinematics and isolation	
leading lepton p_T	$p_T > 20$ GeV
next-to-leading lepton p_T	$p_T > 10$ GeV
additional electrons (muons) p_T	$p_T > 7(5)$ GeV
pseudorapidity of electrons (muons)	$\lvert\eta\rvert < 2.5(2.4)$
p_T sum of all stable particles within $\Delta R < 0.3$ from lepton	$< 0.35 \cdot p_T$
Event topology	
existence of at least two SFOS lepton pairs, where leptons satisfy criteria above	
inv. mass of the Z_1 candidate	$40\,\text{GeV} < m(Z_1) < 120\,\text{GeV}$
inv. mass of the Z_2 candidate	$12\,\text{GeV} < m(Z_2) < 120\,\text{GeV}$
distance between selected four leptons	$\Delta R(\ell_i \ell_j) > 0.02$ for any $i \neq j$
inv. mass of any opposite sign lepton pair	$m(\ell^+ \ell'^-) > 4\,\text{GeV}$
inv. mass of the selected four leptons	$105\,\text{GeV} < m_{4\ell} < 160\,\text{GeV}$
the selected four leptons must originate from the H $\rightarrow 4\ell$ decay	

Analysis strategy: Event selection and reconstruction

✳ Loose leptons (electrons and muons)

✳ Event is required to trigger on at least one of listed HLT paths

✳ Z candidates: any OS-SF pair that satisfies: $12 < m_{\ell\ell}(\gamma) < 120\ \frac{GeV}{c^2}$

✳ ZZ candidates: built by defining Z_1 candidate with $m_{\ell\ell}(\gamma)$ closest to PDG Z-boson mass:

- $m_{Z_1} > 40\ \mathrm{GeV}/c^2$
- $p_T(\ell_1) > 20\ \mathrm{GeV}, p_T(\ell_2) > 10\ \mathrm{GeV}$
- $\Delta R(\eta, \phi) > 0.02$ between each of the four leptons
- $m_{4\ell} > 4\ \mathrm{GeV}/c^2$ for OS pairs
- Reject 4μ *and* $4e$ candidates where the alternate pairing Z_aZ_b satisfies:
  - $|m_{Z_a} - m_Z| < |m_{Z_1} - m_Z|$ AND $m_{Z_b} < 12\ \mathrm{GeV}$

✳ $m_{4\ell} > 70\ \mathrm{GeV}/c^2$

✳ If multiple Z_2s are present, the one with largest p_T sum of the leptons is retained

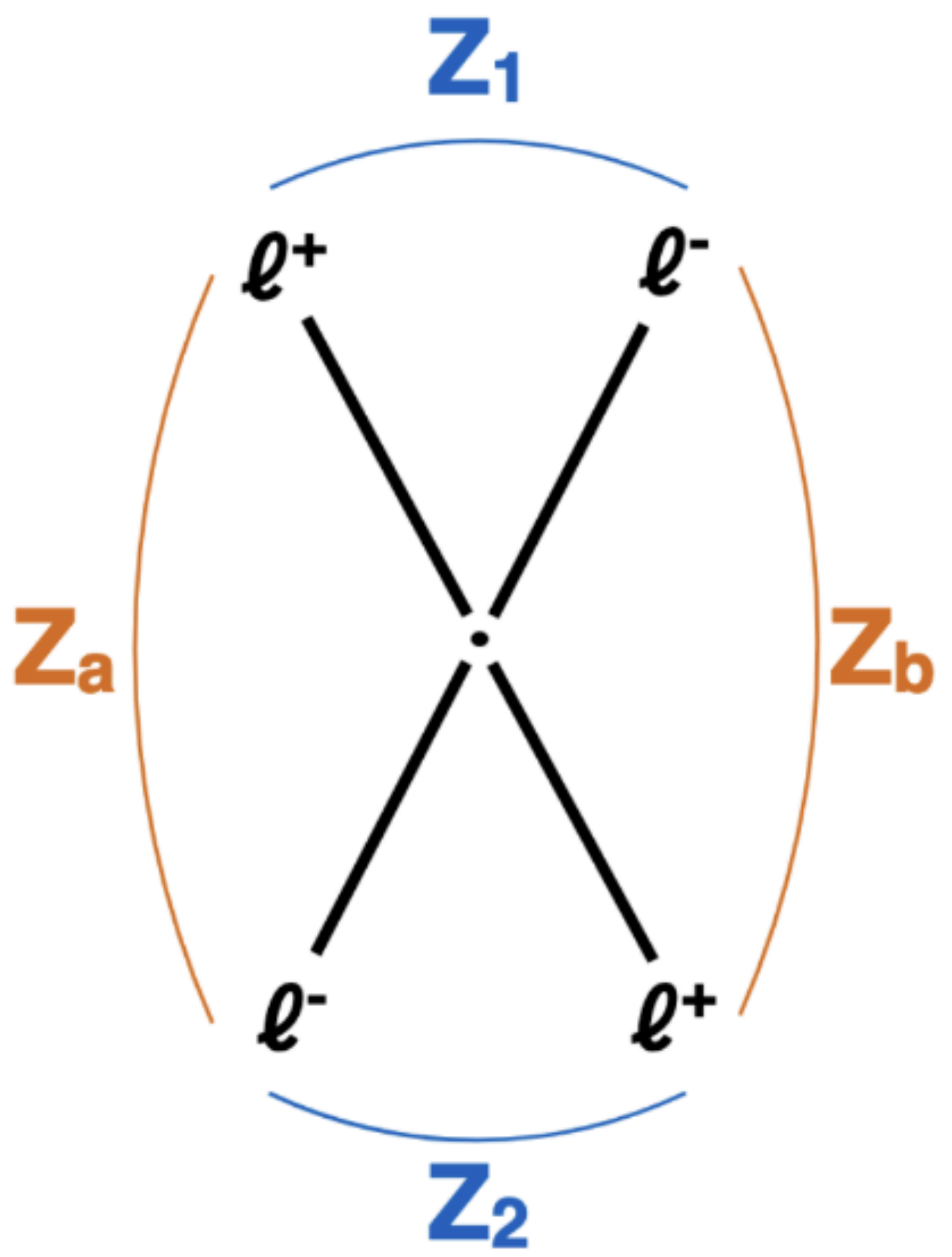

Analysis strategy: Fit procedure

✳Measured by performing a maximum likelihood fit of the signal and background parameterisations to the observed 4ℓ mass distribution

Fiducial signal | Non-resonant signal | Non fiducial signal | Background contribution

$$N^{f,i}_{obs}(m_{4\ell}) = N^{f,i}_{fid}(m_{4\ell}) + N^{f,i}_{nonres}(m_{4\ell}) + N^{f,i}_{nonfid}(m_{4\ell}) + N^{f,i}_{bkg}(m_{4\ell})$$
$$= \left(1 + f^{f,i}_{nonfid}\right) \cdot \sigma^{f,j}_{fid} \cdot \epsilon^{f}_{i,j} \cdot \mathcal{L} \cdot \mathcal{P}_{res}(m_{4\ell}) + N^{f,i}_{nonres} \cdot \mathcal{P}_{nonres}(m_{4\ell}) + N^{f,i}_{bkg} \cdot \mathcal{P}_{bkg}(m_{4\ell}),$$

Parameter of interest ($\sigma^{f,j}_{fid}$)

Probability density function for resonant, non-resonant and background

Process	$4e$	4μ	$2e2\mu$	4ℓ
Signal(m_H =125.38 GeV)	$10.79^{+0.81}_{-1.44}$	$11.74^{+0.21}_{-0.26}$	$30.54^{+1.56}_{-2.63}$	$53.07^{+2.38}_{-4.14}$
nonfid	$0.35^{+0.03}_{-0.05}$	$0.26^{+0.00}_{-0.01}$	$0.32^{+0.02}_{-0.03}$	$0.93^{+0.04}_{-0.08}$
nonres	$0.11^{+0.01}_{-0.02}$	$0.22^{+0.00}_{-0.00}$	$0.33^{+0.02}_{-0.03}$	$0.65^{+0.03}_{-0.05}$
Total signal	$11.25^{+0.85}_{-1.50}$	$12.22^{+0.22}_{-0.27}$	$31.19^{+1.59}_{-2.69}$	$54.65^{+2.45}_{-4.26}$
qqZZ	$13.25^{+1.06}_{-1.96}$	$33.13^{+1.80}_{-1.78}$	$38.70^{+2.41}_{-4.06}$	$85.07^{+4.59}_{-7.20}$
ggZZ	$1.89^{+0.22}_{-0.34}$	$3.90^{+0.46}_{-0.40}$	$3.95^{+0.44}_{-0.56}$	$9.74^{+1.08}_{-1.24}$
ZX	$4.34^{+1.20}_{-1.54}$	$14.23^{+6.49}_{-2.22}$	$17.16^{+3.27}_{-3.60}$	$35.73^{+7.61}_{-4.35}$
Sum of backgrounds	$19.48^{+1.47}_{-2.97}$	$51.26^{+7.65}_{-2.30}$	$59.80^{+3.89}_{-5.84}$	$130.54^{+9.38}_{-8.27}$
Total expected	$30.72^{+2.10}_{-4.29}$	$63.48^{+7.73}_{-2.36}$	$90.99^{+4.67}_{-8.03}$	$185.19^{+9.66}_{-11.91}$

Results: Inclusive cross section $H \rightarrow ZZ \rightarrow 4\ell$

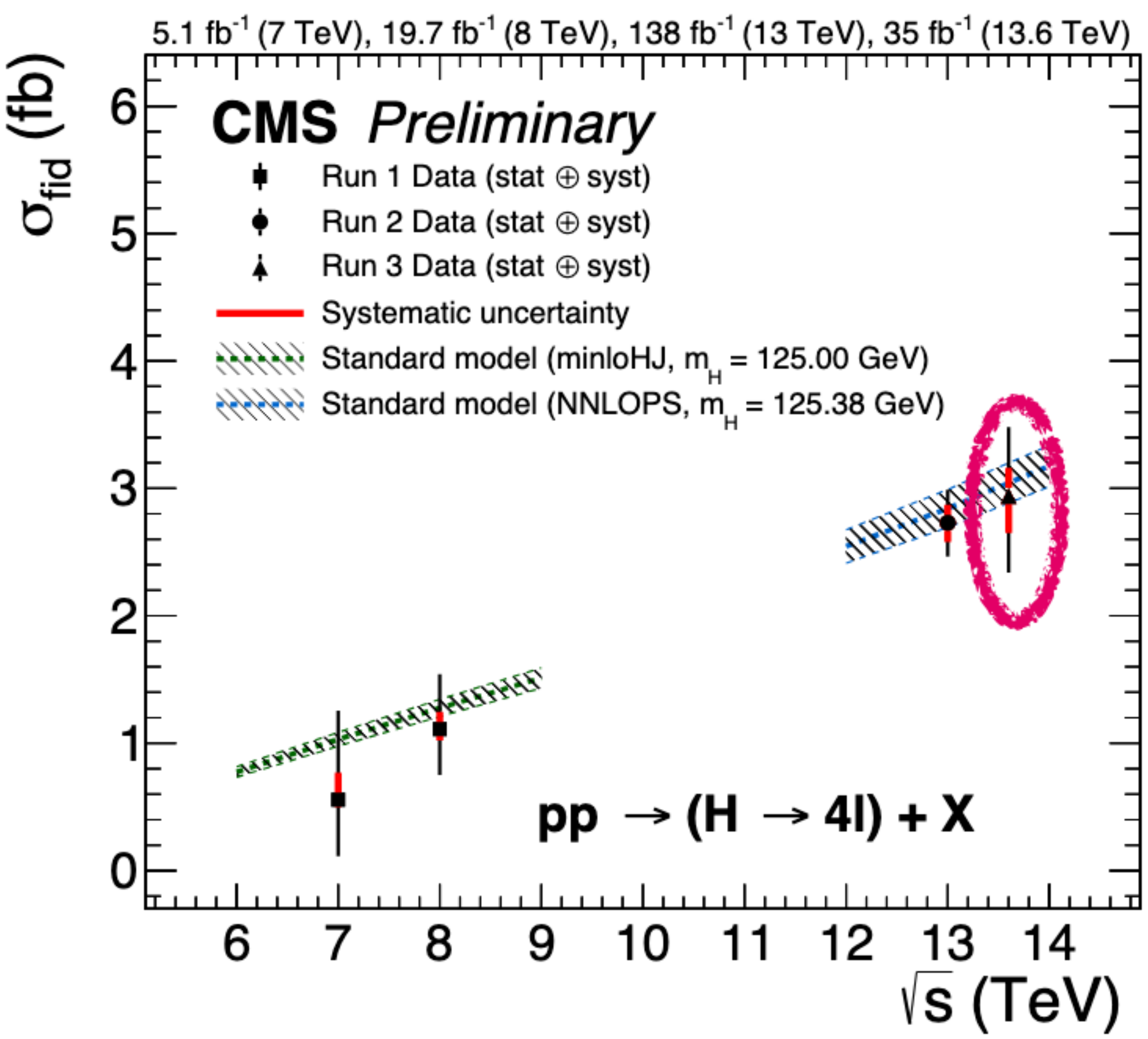

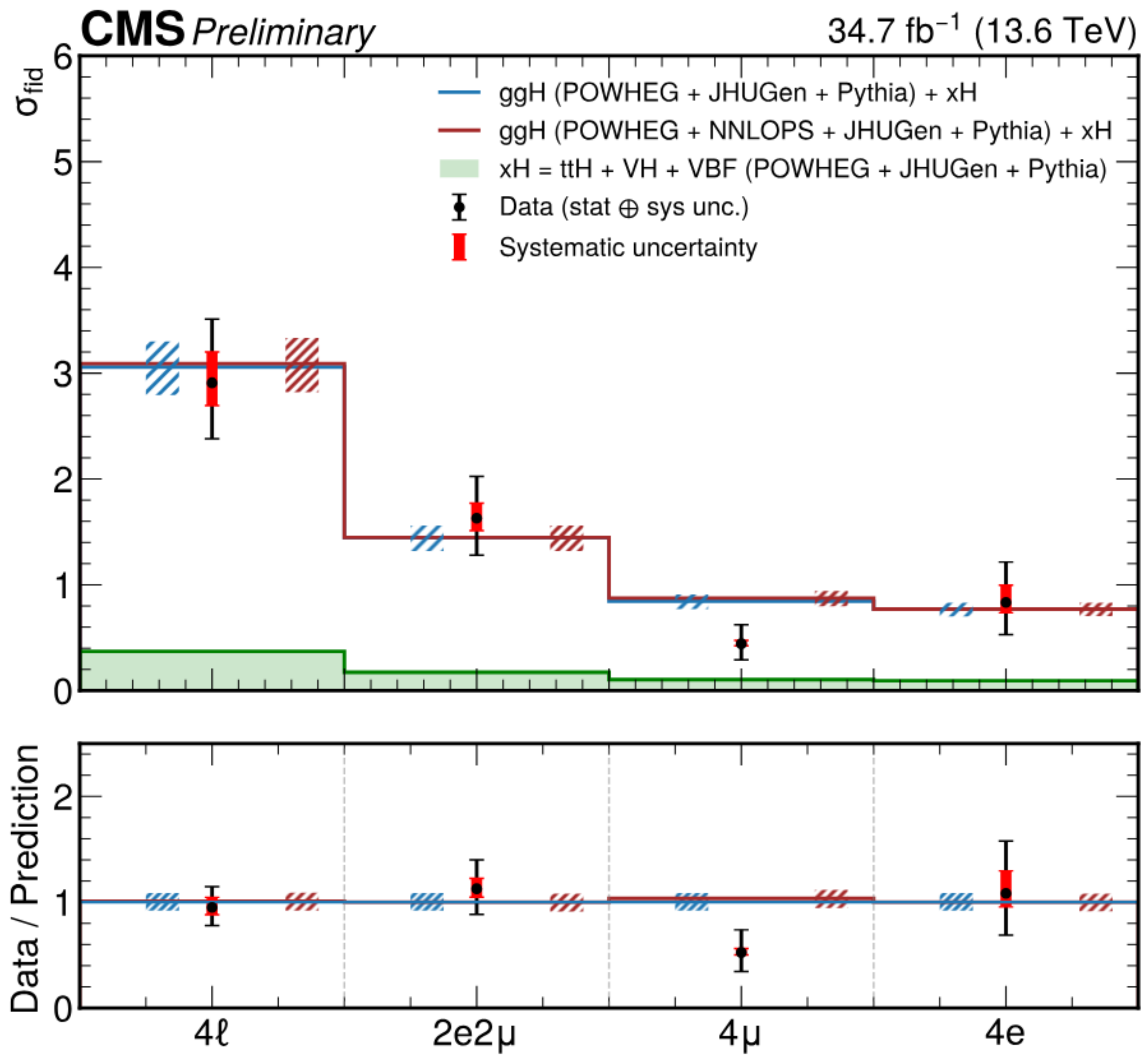

Measurements per lepton category consistent with each other

- ✴Most relevant systematic: Electron efficiency
- ✴Measured inclusive cross section

$$\sigma_{\mathrm{fid}} = 2.94^{+0.53}_{-0.49}\ (\mathrm{stat.})^{+0.29}_{-0.22}\ (\mathrm{syst.})\ \mathrm{fb}$$

Results: Differential cross section $H \to ZZ \to 4\ell$

✳ Fiducial differential cross sections are measured in bins of some variables (e.g. Higgs kinematics, jet properties, decay variables)

✳ Two variables studied: p_T^H , $|y^H|$ (coarse binning w.r.t. Run2)

- In agreement with SM
- Systematics dominated by Electron efficiency

✳ Full Run 3 dataset → more granular binning expected

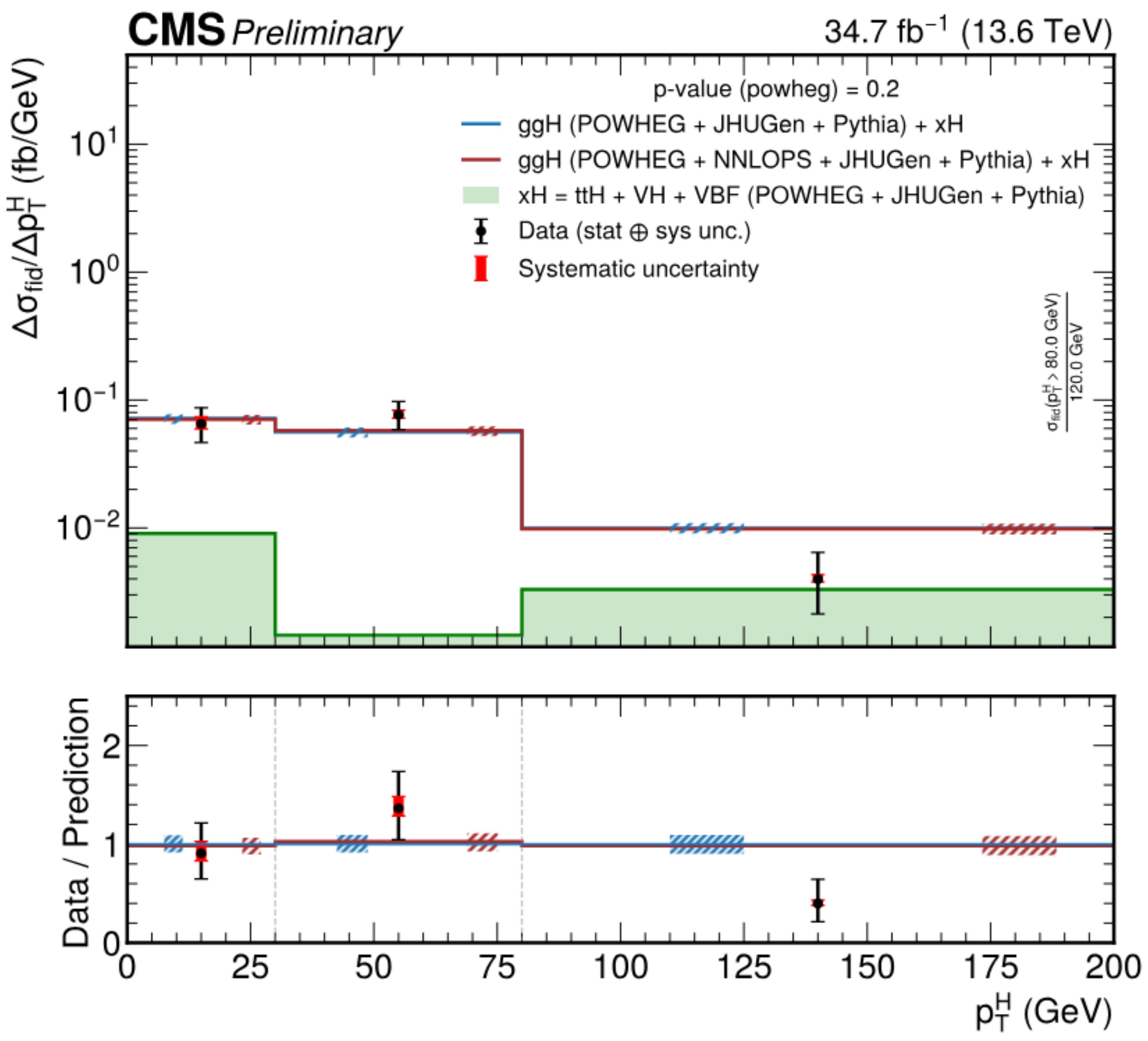

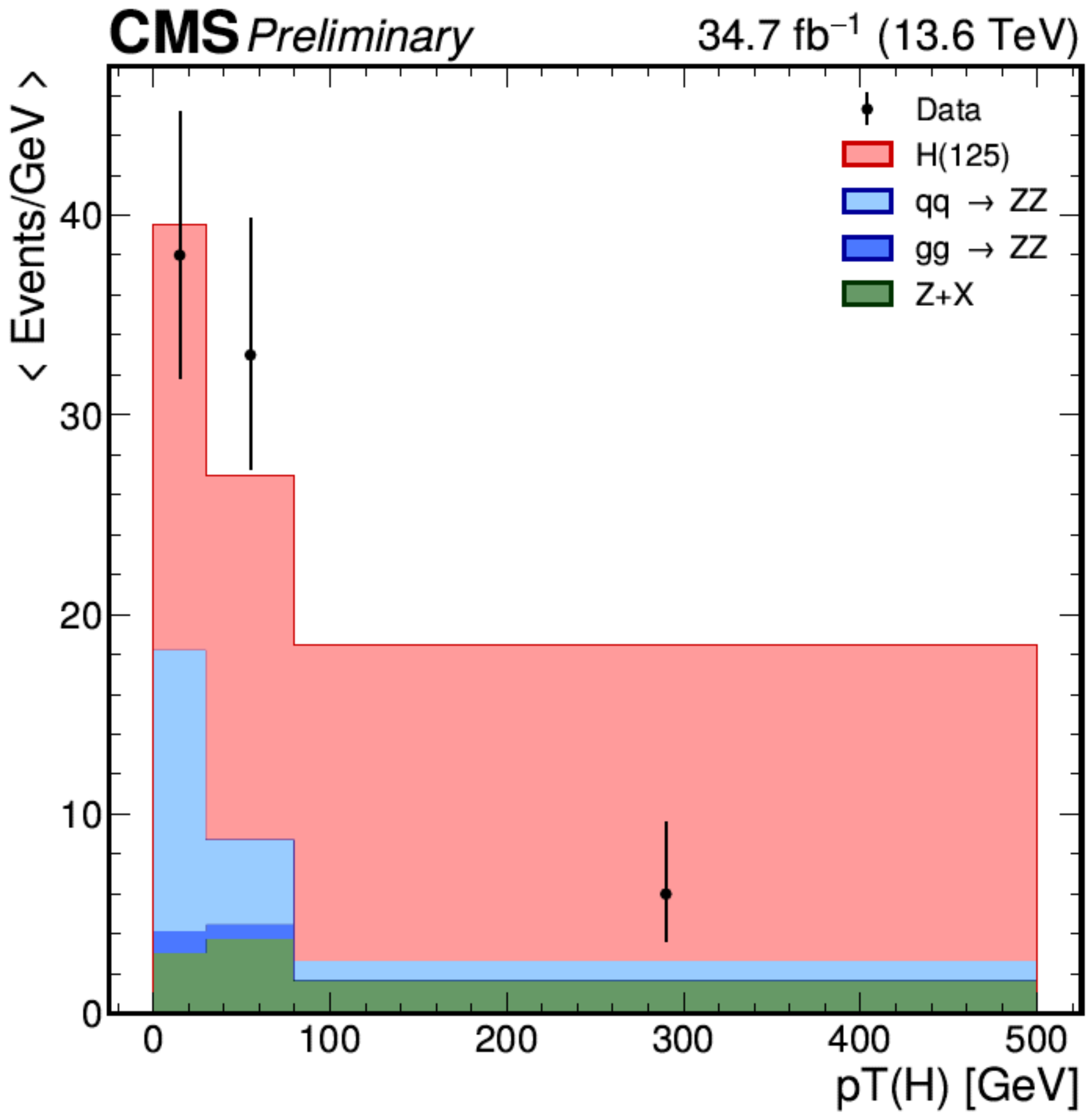

Results: Differential cross section $H \to ZZ \to 4\ell$

CMS-PAS-HIG-24-013

✳ Fiducial differential cross sections are measured in bins of some variables (e.g. Higgs kinematics, jet properties, decay variables)

✳ Two variables studied: p_T^H , $|y^H|$ (coarse binning w.r.t. Run2)

- In agreement with SM
- Systematics dominated by Electron efficiency

✳ Full Run 3 dataset → more granular binning expected

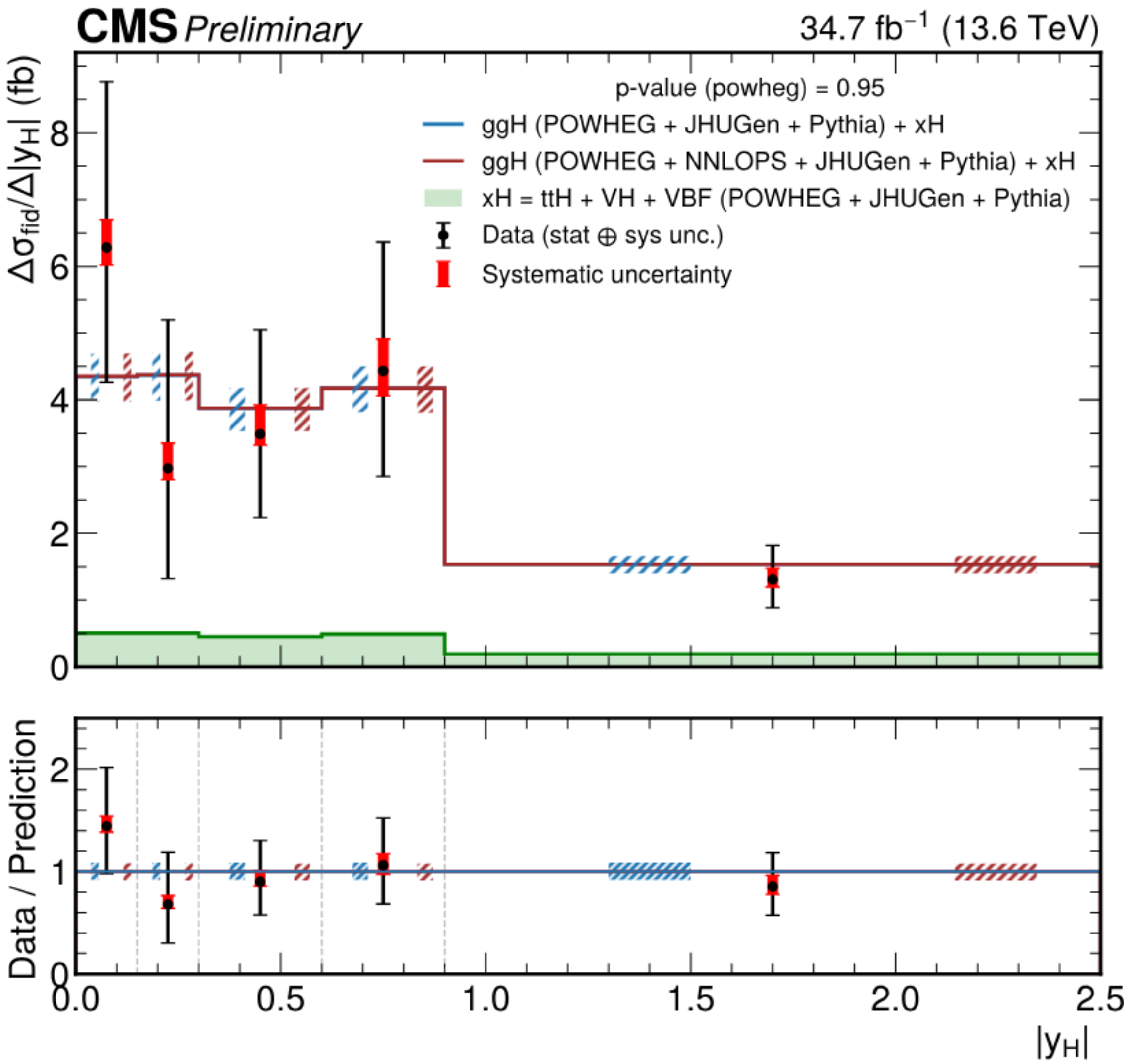

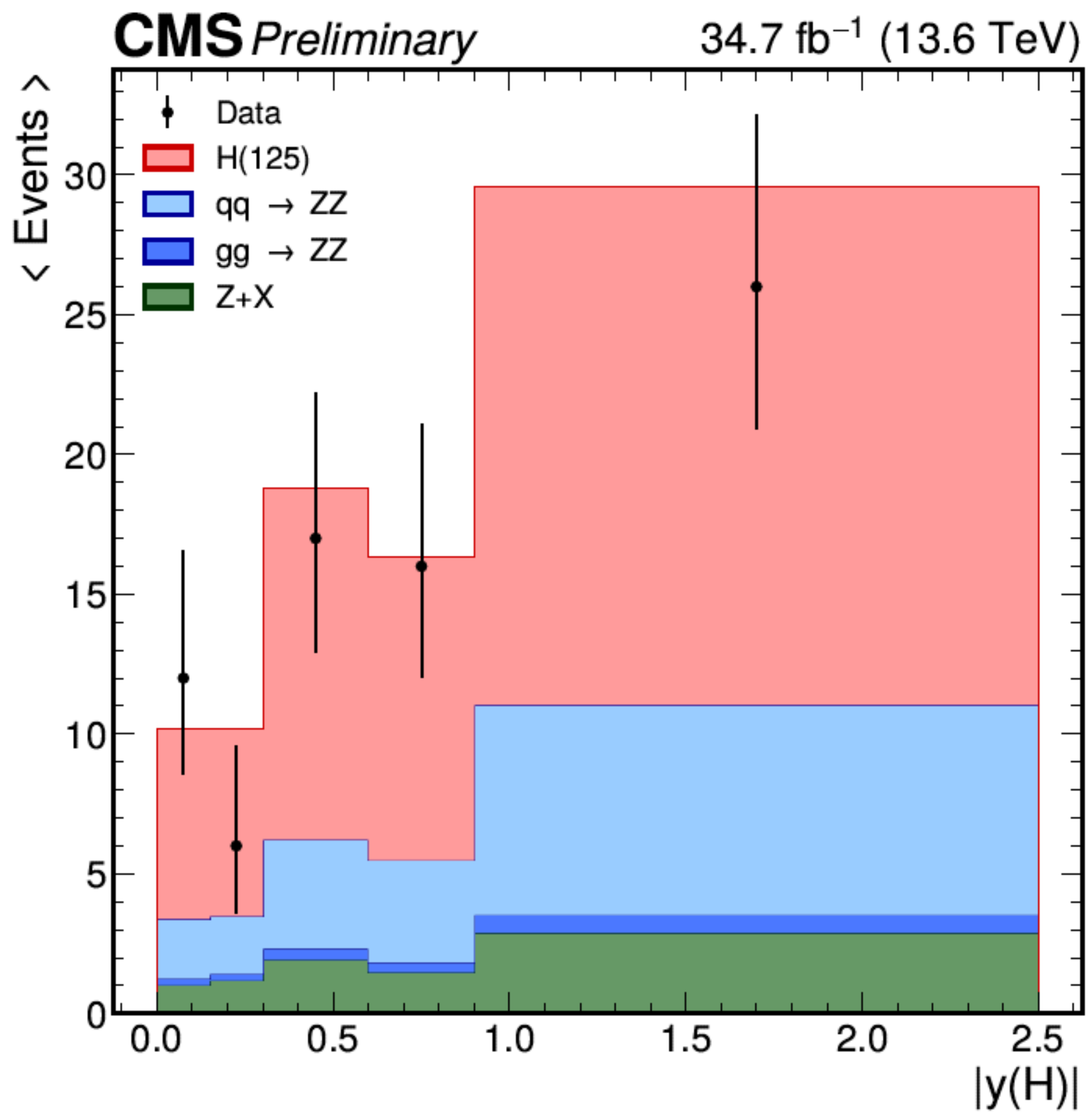

Summary

✳Presented the recent Higgs cross section results *measured* in $H \to ZZ \to 4\ell$ decay channel

- Inclusive and differential measurements reported
- Early Run3 data from CMS $(34.7\ fb^{-1})$
  - See backup slides for recent Run 2 results $(138\ fb^{-1})$

✳Full Run 3 data would provide us the opportunity to explore more fine granularity to such measurements (for extensive set of 1D and 2D observables, interpretations, combinations, …..)

- $2023 + 2024$ recorded data already been certified by CMS $(136.16\ fb^{-1})$
- Luminosity expected in $2025 + 2026$ up to $220\ fb^{-1}$

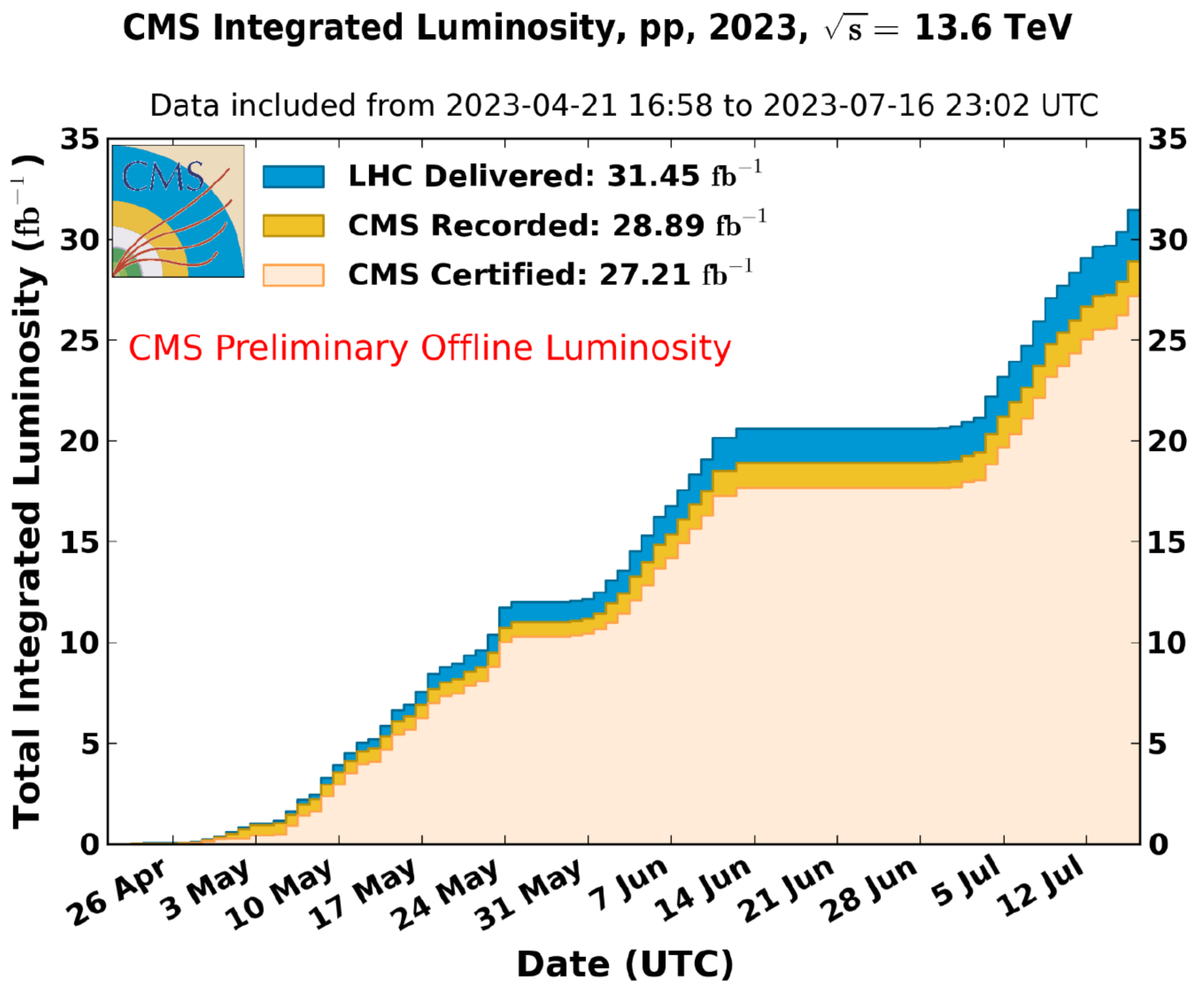

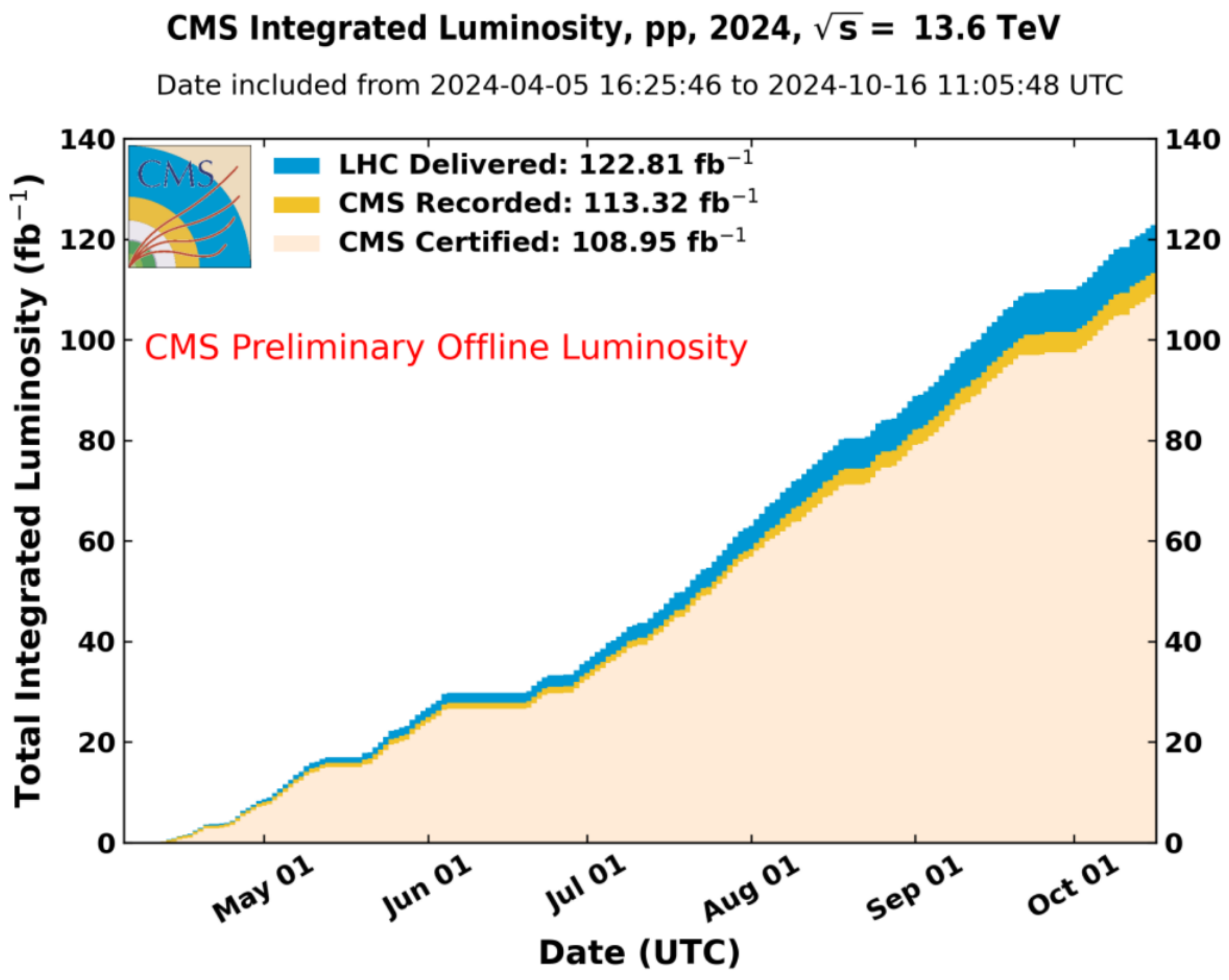


Thank you

BACKUP SLIDES

Strategy for Run3 analyses release

Short term *(during 2025)* : 2022+2023 publications *(possibly in combination with Run2)*

Medium term *(from Moriond26)* : include 2024 data *(for as many analyses as possible)*

Long term *(from Moriond27)* : full Run3

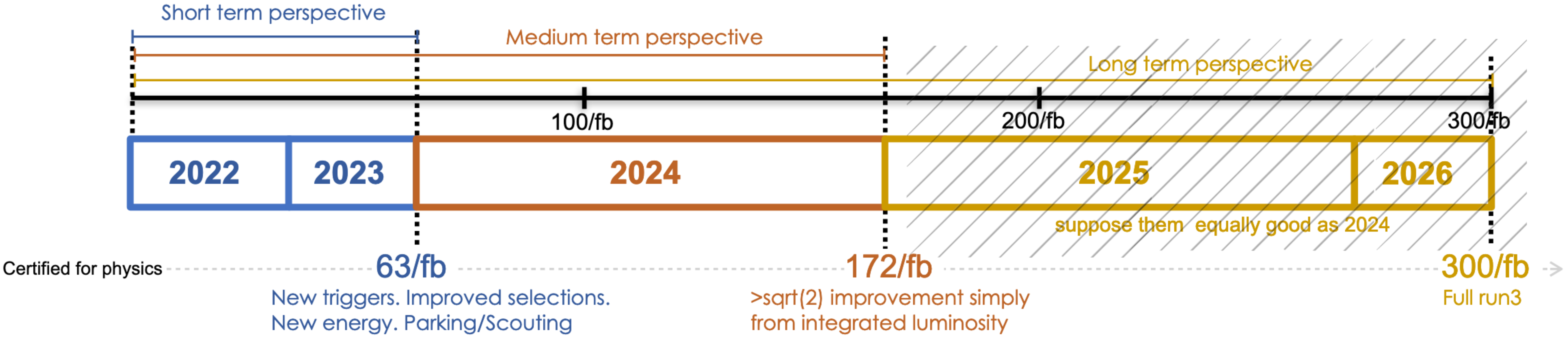

$$H \to ZZ \to 4\ell$$

Full Run2 strategy and results

Event selection and reconstructions

✳Z candidate

◉Any OS-SF pair that satisfies $12 < m_{ll(\gamma)} < 120$ GeV

✳Build all possible ZZ candidates defined as pairs of non-overlapping Z candidate;

define Z_1 candidate with $m_{ll(\gamma)}$ closest to the PDG m(Z) mass

◉$m_{Z1} > 40$ GeV; $P_T(l1) > 20$ GeV; $P_T(l2) > 10$ GeV

◉ $\Delta R > 0.02$ between each of the four leptons

◉$m_{ll} > 4$ GeV for OS pairs (regardless of flavor)

◉Reject 4μ and 4e candidates where the alternative pair Z_aZ_b satisfies

$\left| m_{Za} - m_Z \right| < \left| m_{Z1} - m_Z \right|$ and $m_{Zb} < 12$ GeV

◉$m_{4l} > 70$ GeV

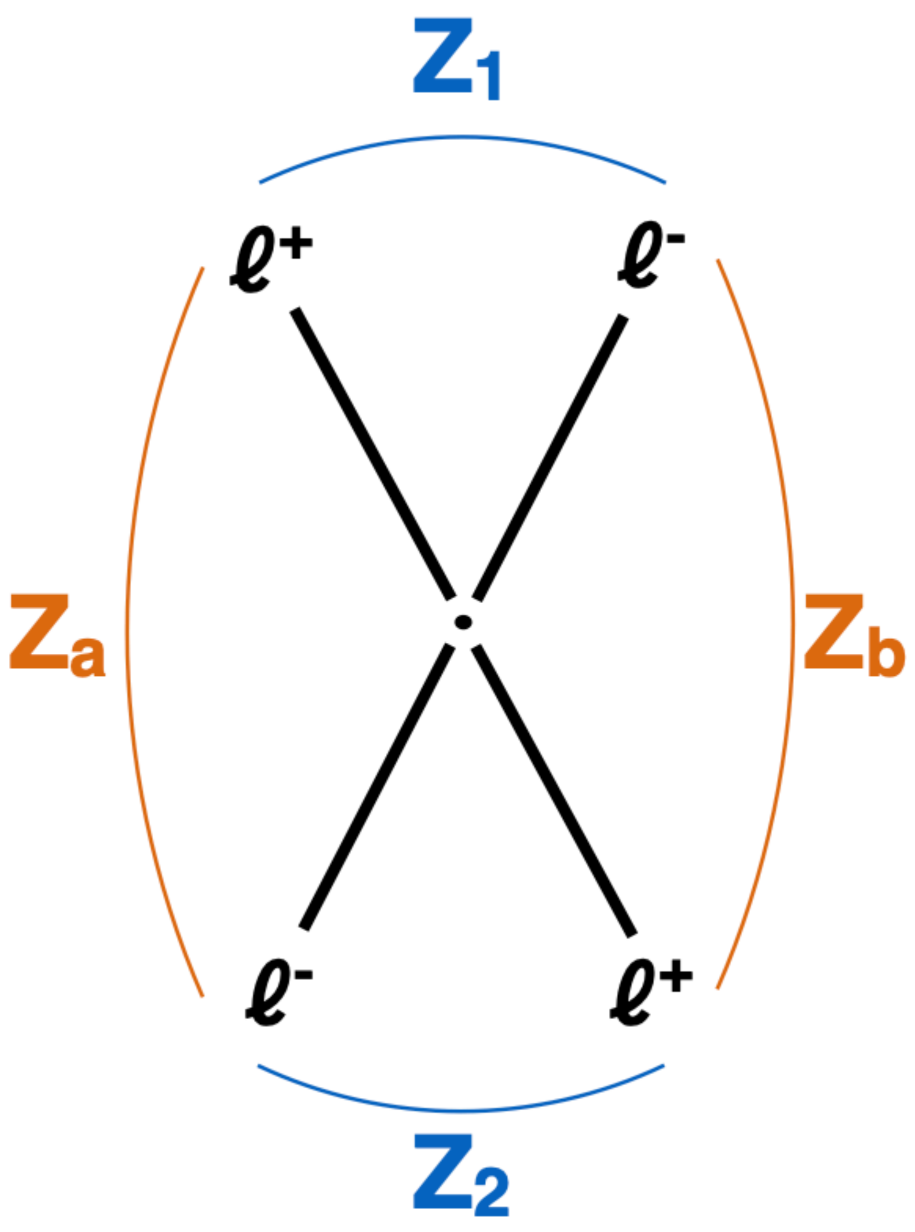

✳If more than one ZZ candidate is left, take the one with Z_1 mass closest to m_Z and

the Z_2 from the candidates whose lepton give higher pT sum.

EPJC81(2021)488

Background Estimation

✳Irreducible background

- ◉Production of ZZ via $q\bar{q}$ annihilation or gluon fusion
- ◉Estimated using simulation

✳Reducible background

- ◉Light flavor hadrons misidentified as leptons
- ◉Heavy flavor jets produce secondary leptons through the decay of heavy flavor mesons
- ◉Two independent methods used to estimated Z+X background: OS and SS
  - Fake rates calculated in Z+l control region
  - Z+X yields estimated in orthogonal regions of Z+ll control region
  - Final estimate combination of 2 methods
- ◉Templates are built from the control regions in data

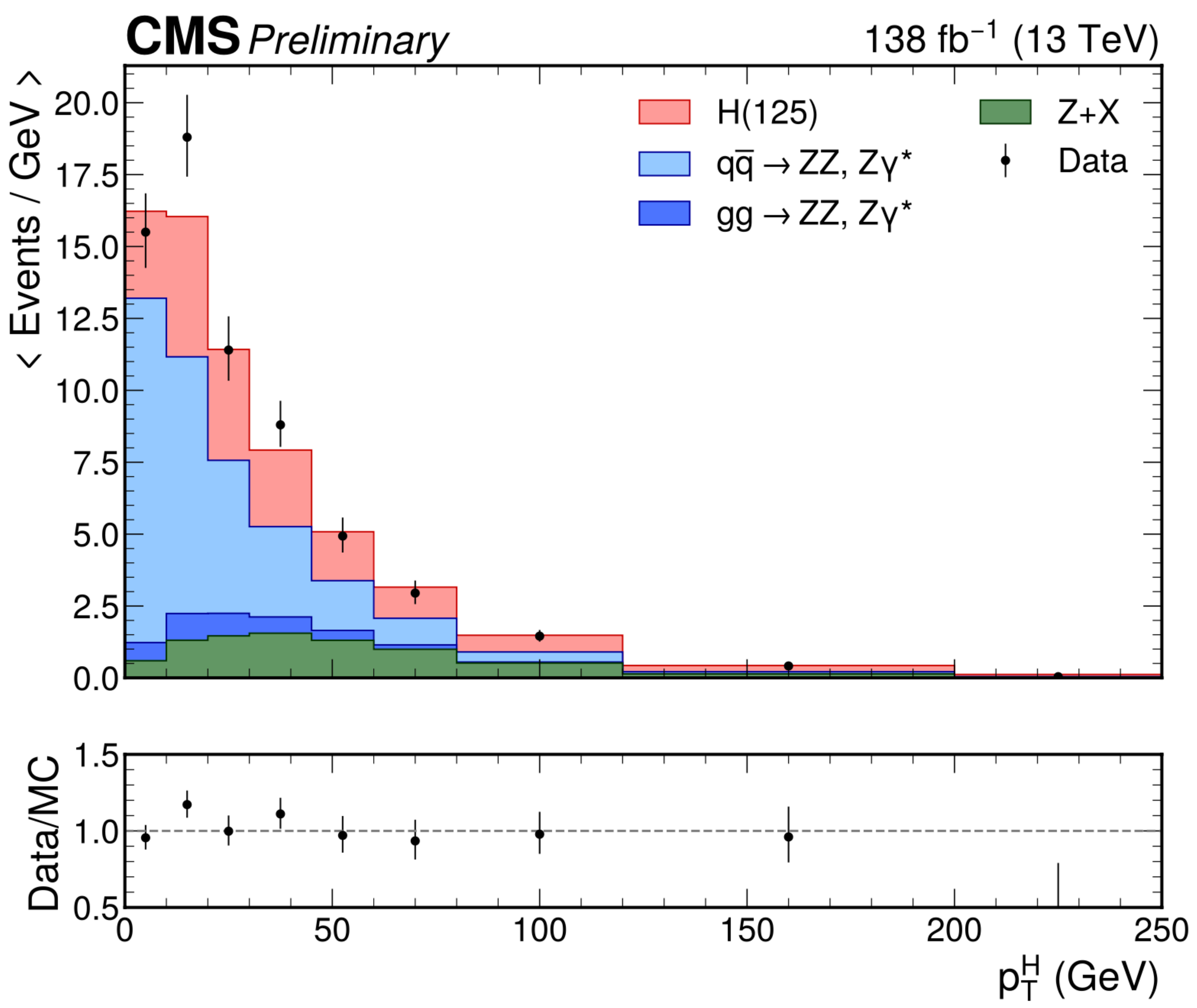

EPJC81(2021)488

Systematic Uncertainties

✳Experimental uncertainties

◉Integrated luminosity

◉Lepton identification and reconstruction efficiency → →

◉Reducible background

◉Lepton scale and resolution

◉Jet energy scale

✳Theoretical uncertainties

◉**QCD uncertainty** from renormalization and factorization scale

◉Uncertainty on the Choice of **PDF set** is determined following the PDF4LHC recommendations

◉Uncertainty of 2% on H → 4l **branching ratio** affects only signal yields

The uncertainties of lepton reconstruction and selection range for
- 4μ channel 0.8 - 1.9%
- 4e channel 6.5 - 11%

A reduction of about 5% in the 4e uncertainties thanks to a dedicated RMS method.

EPJC81(2021)488

Summary of inclusive theory uncertainties	
QCD scale (gg)	$\pm$ 3.9 %
PDF set (gg)	$\pm$ 3.2 %
gg $\rightarrow$ ZZ k-factor (gg)	$\pm$ 10 %
QCD scale ($q\bar{q} \rightarrow$ ZZ)	+3.2/-4.2 % %
PDF set ($q\bar{q} \rightarrow$ ZZ)	+3.1/-3.4 %
Electroweak corrections ($q\bar{q} \rightarrow$ ZZ)	$\pm$ 0.1 %
QCD scale (VBF)	+0.4/-0.3 %
PDF set (VBF)	$\pm$ 2.1 %
QCD scale (WH)	+0.5/-0.7 %
PDF set (WH)	$\pm$ 1.9 %
QCD scale (ZH)	+3.8/-3.1 %
PDF set (ZH)	$\pm$ 1.6 %
QCD scale ($t\bar{t}$H)	+5.8/-9.2 %
PDF set ($t\bar{t}$H)	$\pm$ 3.6 %
BR(H $\rightarrow$ ZZ $\rightarrow 4\ell$)	2 %

Common experimental uncertainties			
	2016	2017	2018
Luminosity uncorrelated	1 %	2 %	1.5 %
Luminosity corr 16 17 18	0.6 %	0.9 %	2 %
Luminosity corr 17 18	-	0.6 %	0.2 %
Lepton id/reco efficiencies	0.7–10 %	0.6 – 8.5 %	0.6 – 9.5 %
Background related uncertainties			
Reducible background (Z+X)	25 – 43 %	23 – 36 %	24 –36 %
Signal related uncertainties			
Lepton energy scale	0.01%(μ) - 0.06%(e)	0.01%(μ) - 0.06%(e)	0.01%(μ) - 0.06%(e)
Lepton energy resolution	3%(μ) - 10%(e)	3%(μ) - 10%(e)	3%(μ) - 10%(e)

Fiducial/Differential Cross Section measurement

EPJC81(2021)488

- Definition of the fiducial phase space of $H \to ZZ \to 4l$

$$\sigma_i = \frac{N_{reco,\,i}}{C_i * A_i * L * B} \to \to \sigma_{fid,\,i} * B = \frac{N_{reco,\,i}}{C_i * L}$$

- Number of events of different final state f and different year y in the given bin i are expressed as a function of 4l invariable mass

$$N^{f,i,y}_{\mathrm{obs}}(m_{4\ell}) = N^{f,i,y}_{\mathrm{fid}}(m_{4\ell}) + N^{f,i,y}_{\mathrm{nonfid}}(m_{4\ell}) + N^{f,i,y}_{\mathrm{nonres}}(m_{4\ell}) + N^{f,i,y}_{\mathrm{bkg}}(m_{4\ell})$$
$$= \sum_{j}^{\mathrm{genBin}} \epsilon^{f,y}_{i,j,y} \cdot (1 + f^{f,i,y}_{\mathrm{nonfid}}) \cdot \sigma^{f,j,y}_{\mathrm{fid}} \cdot \mathcal{L} \cdot \mathcal{P}^{f,y}_{\mathrm{res}}(m_{4\ell})$$
$$+ N^{f,i,y}_{\mathrm{nonres}} \cdot \mathcal{P}^{f,y}_{\mathrm{nonres}}(m_{4\ell}) + N^{f,i,y}_{\mathrm{bkg}} \cdot \mathcal{P}^{f,i,y}_{\mathrm{bkg}}(m_{4\ell})$$

- Fiducial + non-fiducial resonances signal contribution:
  - Shape is described by double-sided Crystal Ball function.
  - Normalization is proportional to the fiducial cross section.
- Non-resonant signal contribution
  - Arises from WH, ZH ttH where one of the leptons from Higgs is lost or not selected.
  - Modeled by Landau distribution
  - Treated as background

Requirements for the $H \to 4\ell$ fiducial phase space

Lepton kinematics and isolation	
Leading lepton p_T	$p_T > 20\,\mathrm{GeV}$
Sub-leading lepton p_T	$p_T > 10\,\mathrm{GeV}$
Additional electrons (muons) p_T	$p_T > 7(5)\,\mathrm{GeV}$
Pseudorapidity of electrons (muons)	$\lvert\eta\rvert < 2.5\ (2.4)$
Sum of scalar p_T of all stable particles within $\Delta R < 0.3$ from lepton	$< 0.35 p_T$
Event topology	
Existence of at least two same-flavor OS lepton pairs, where leptons satisfy criteria above	
Inv. mass of the Z_1 candidate	$40 < m_{Z_1} < 120\,\mathrm{GeV}$
Inv. mass of the Z_2 candidate	$12 < m_{Z_2} < 120\,\mathrm{GeV}$
Distance between selected four leptons	$\Delta R(\ell_i, \ell_j) > 0.02$ for any $i \neq j$
Inv. mass of any opposite sign lepton pair	$m_{\ell^+\ell'^-} > 4\,\mathrm{GeV}$
Inv. mass of the selected four leptons	$105 < m_{4\ell} < 160\,\mathrm{GeV}$

Results

Inclusive fiducial cross section

Differential production observables

p_T^H $|y_H|$ p_T^{j1} N_{jets}

p_T^{Hj} m_{Hjj} p_T^{j2} T_B^{max} T_C^{max}

p_T^{Hjj} m_{jj} $|\Delta\eta_{jj}|$ $|\Delta\phi_{jj}|$

Differential decay observables

m_{Z1} m_{Z2} Φ Φ_1

$\cos(\theta_1)$ $\cos(\theta*)$ $\cos(\theta_2)$

D_{0-}^{dec} D_{CP}^{dec} D_{0h+}^{dec} $D_{\Lambda1}^{dec}$ $D_{\Lambda1}^{Z\gamma,dec}$ D_{int}^{dec}

Double-differential observables

T_C^{max} vs p_T^H

m_{Z1} vs m_{Z2}

N_{jet} vs p_T^H

p_T^H vs p_T^{Hj}

$|y_H|$ vs p_T^H

p_T^{j1} vs p_T^{j2}

Inclusive fiducial cross section

Differential production observables

p_T^H $|y_H|$ p_T^{j1} N_{jets}

p_T^{Hj} m_{Hjj} p_T^{j2} T_B^{max} T_C^{max}

p_T^{Hjj} m_{jj} $|\Delta\eta_{jj}|$ $|\Delta\phi_{jj}|$

Differential decay observables

m_{Z1} m_{Z2} Φ Φ_1

$\cos(\theta_1)$ $\cos(\theta^*)$ $\cos(\theta_2)$

D_{0-}^{dec} D_{CP}^{dec} D_{0h+}^{dec} $D_{\Lambda1}^{dec}$ $D_{\Lambda1}^{Z\gamma,dec}$ D_{int}^{dec}

Double-differential observables

T_C^{max} vs p_T^H m_{Z1} vs m_{Z2}

N_{jet} vs p_T^H p_T^H vs p_T^{Hj}

$|y_H|$ vs p_T^H p_T^{j1} vs p_T^{j2}

Results: Inclusive

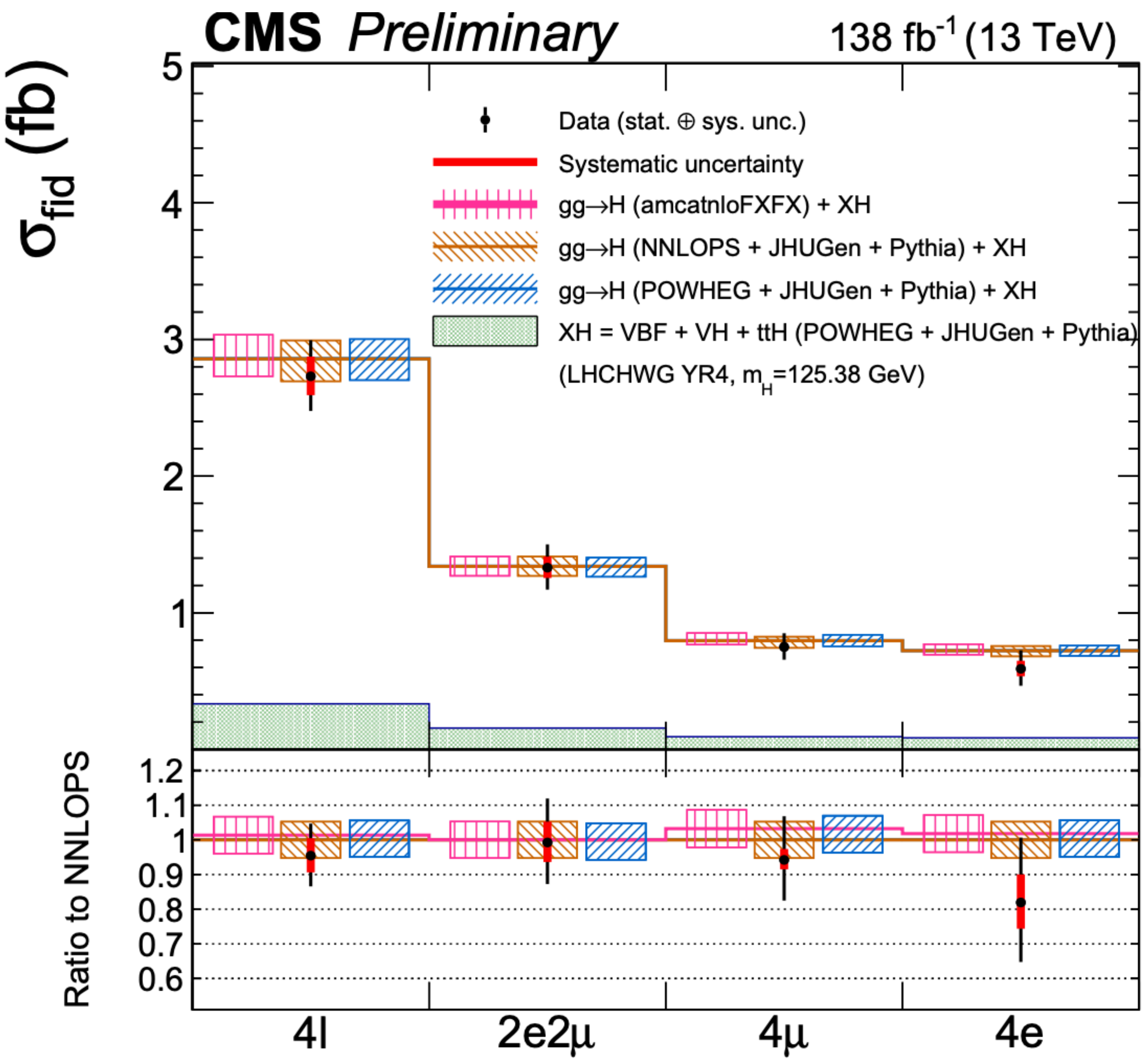

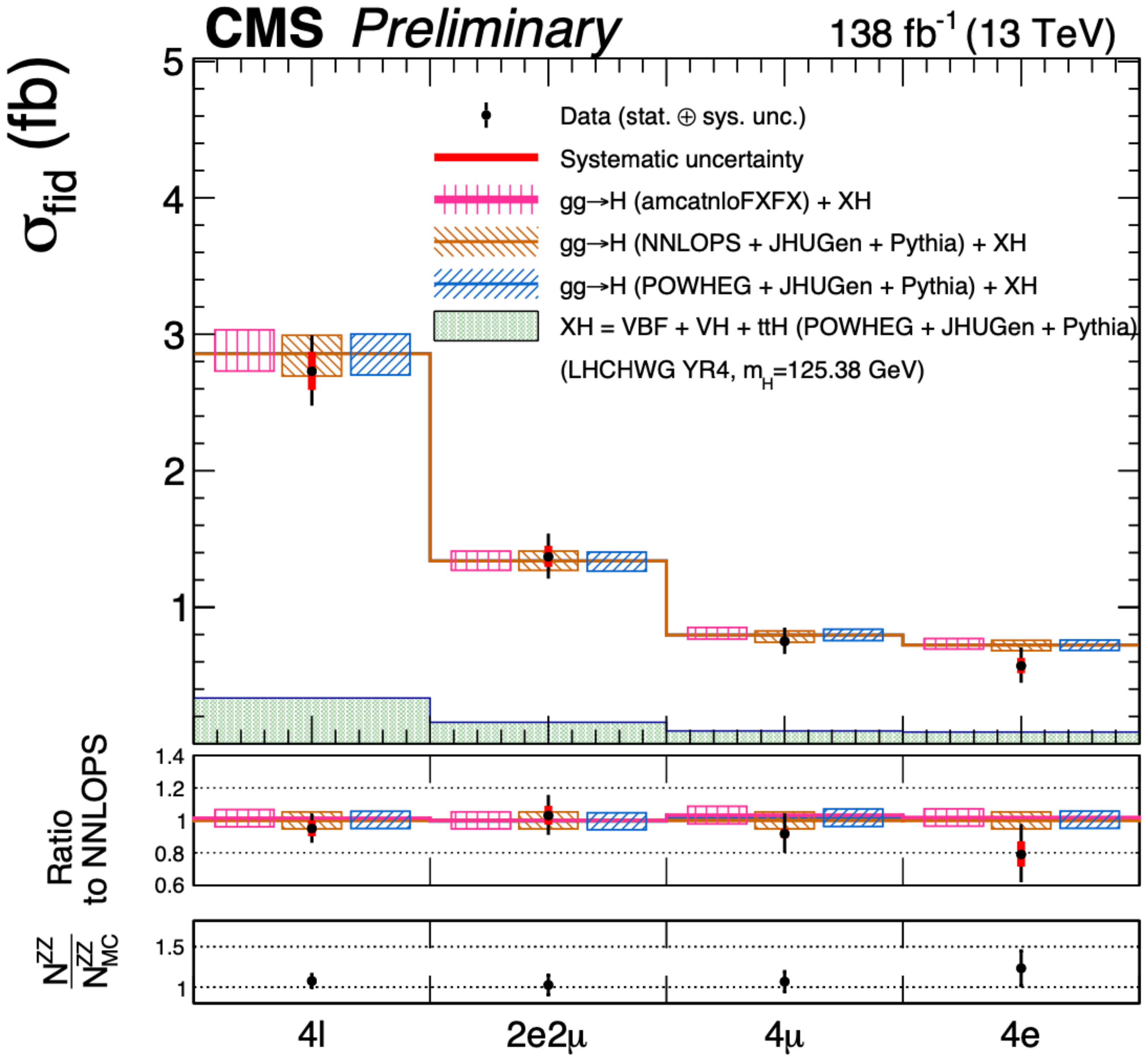

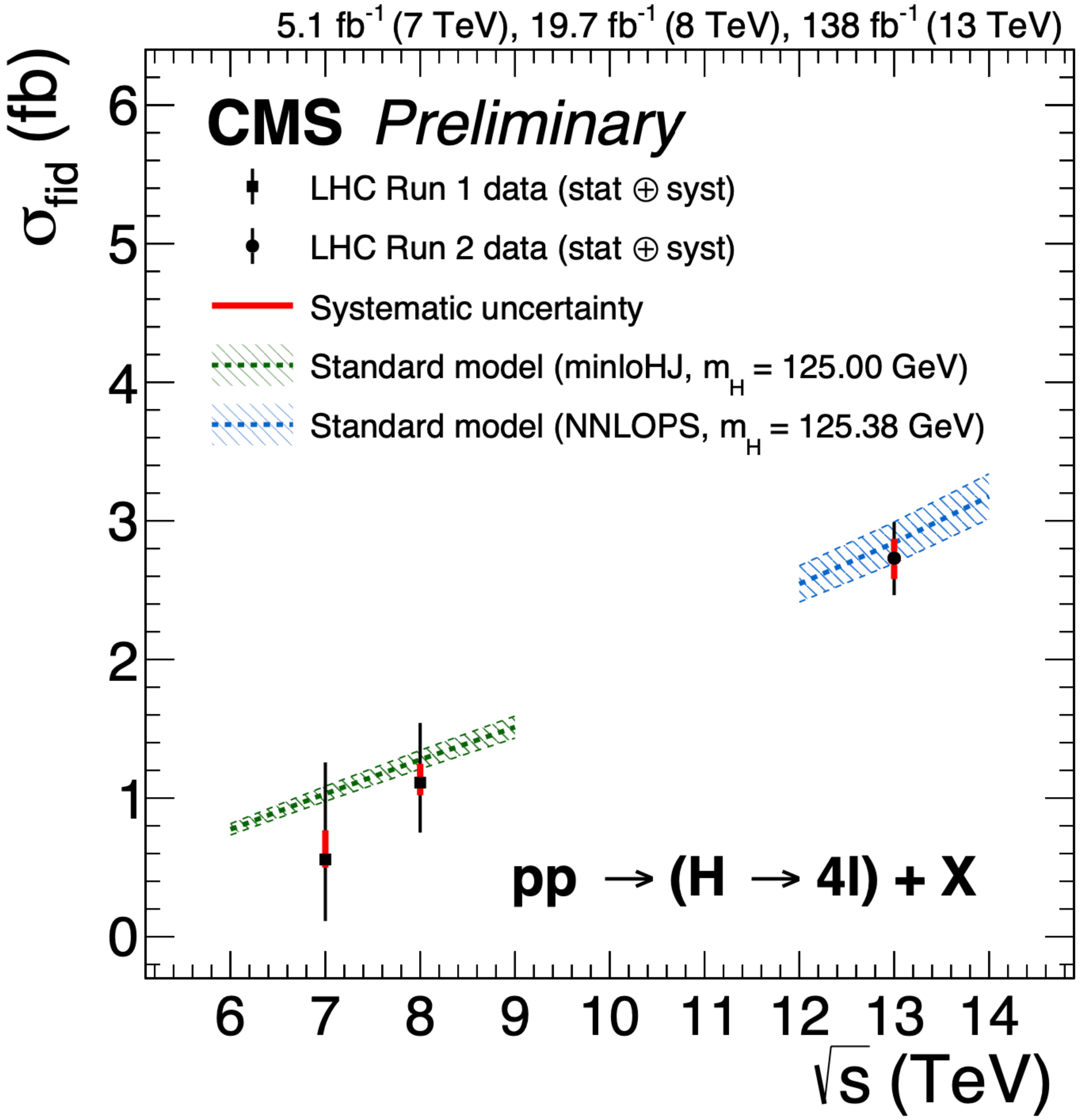

- ✳ Standard approach (left): extract both the shape and the normalisation of the ZZ irreducible background from the simulation
- ✳ **Alternative strategy (middle): Measuring together the inclusive fiducial cross section and the ZZ normalisation**
  - ◉ Remove the impact of nuisances on ZZ normalisation
  - ◉ Being sensitive to BSM effects in the background
  - ◉ Reduction of the systematic component on the XS wrt standard approach, but not yet enough number of events to profit from this method for **differential** measurements

Results: Inclusive (all channels)

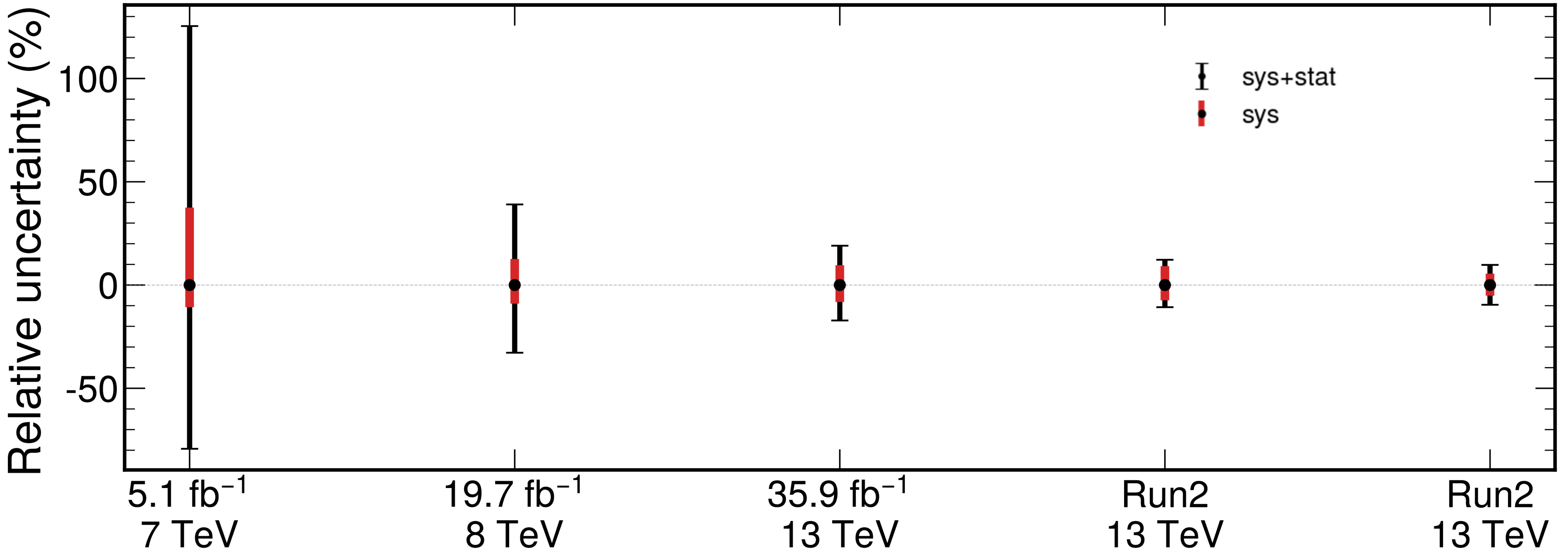

JHEP04(2016)005 *JHEP04(2016)005* *JHEP11(2017)047* *EPJC81(2021)488* [*CMS-PAS-HIG-21-009*]

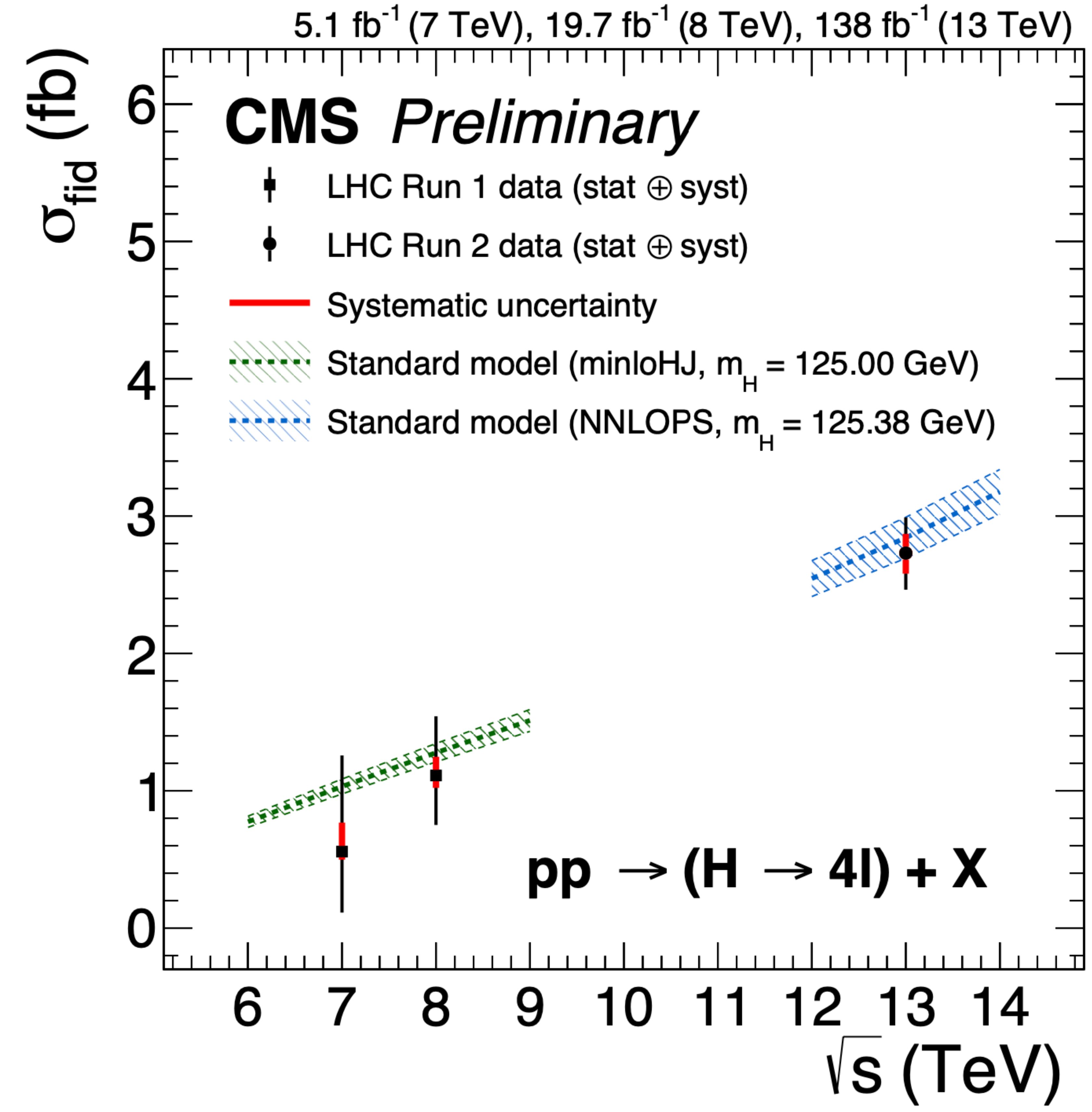

Results: Inclusive (all channels)

- Precision @ **10%**
- **40% decrease of the systematic component** due to the reduction of the main lepton nuisances
- **Electron-related nuisances** are the leading contribution to the systematic uncertainty but their value is halved
- Systematic component at the same level of the theoretical precision

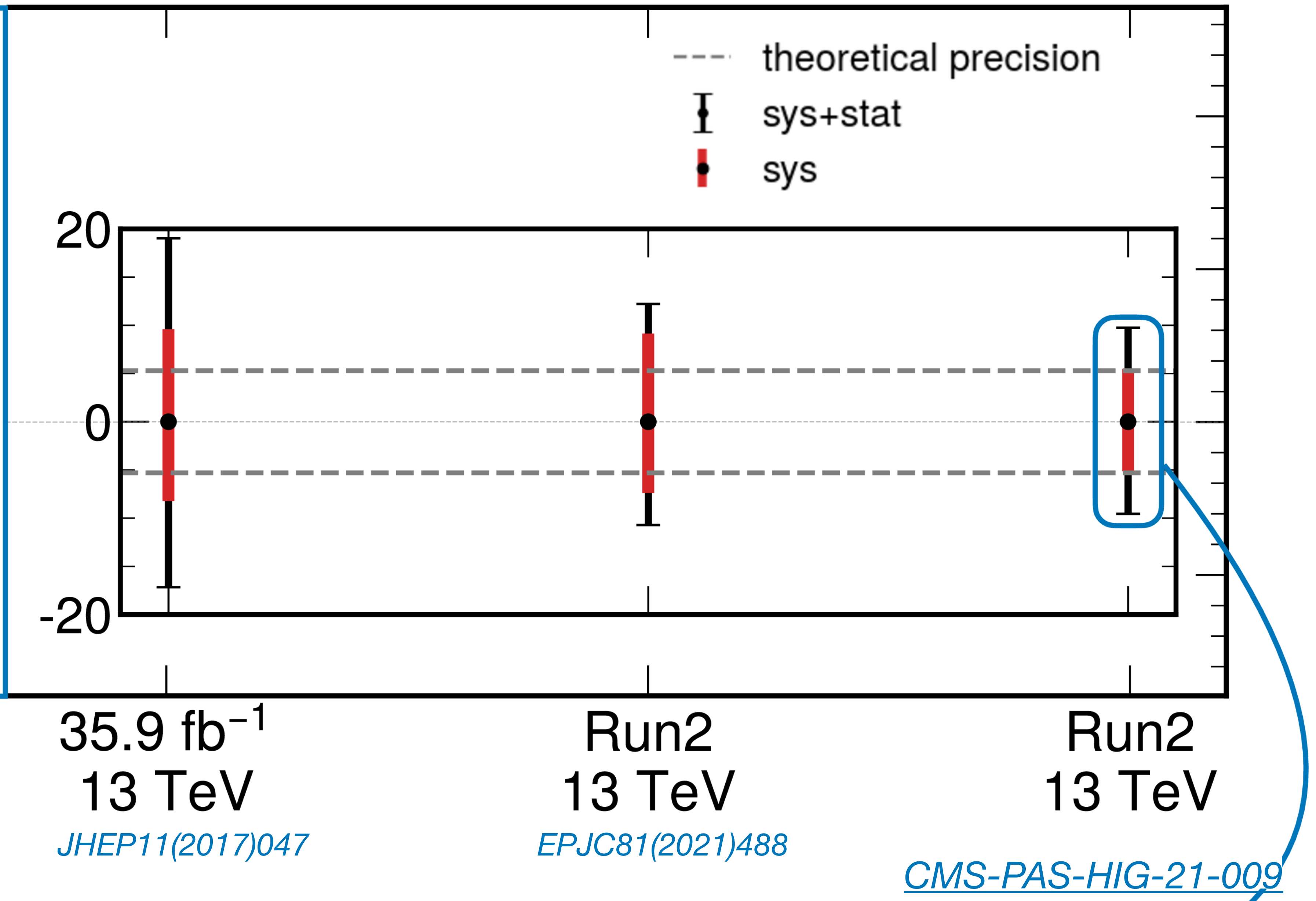

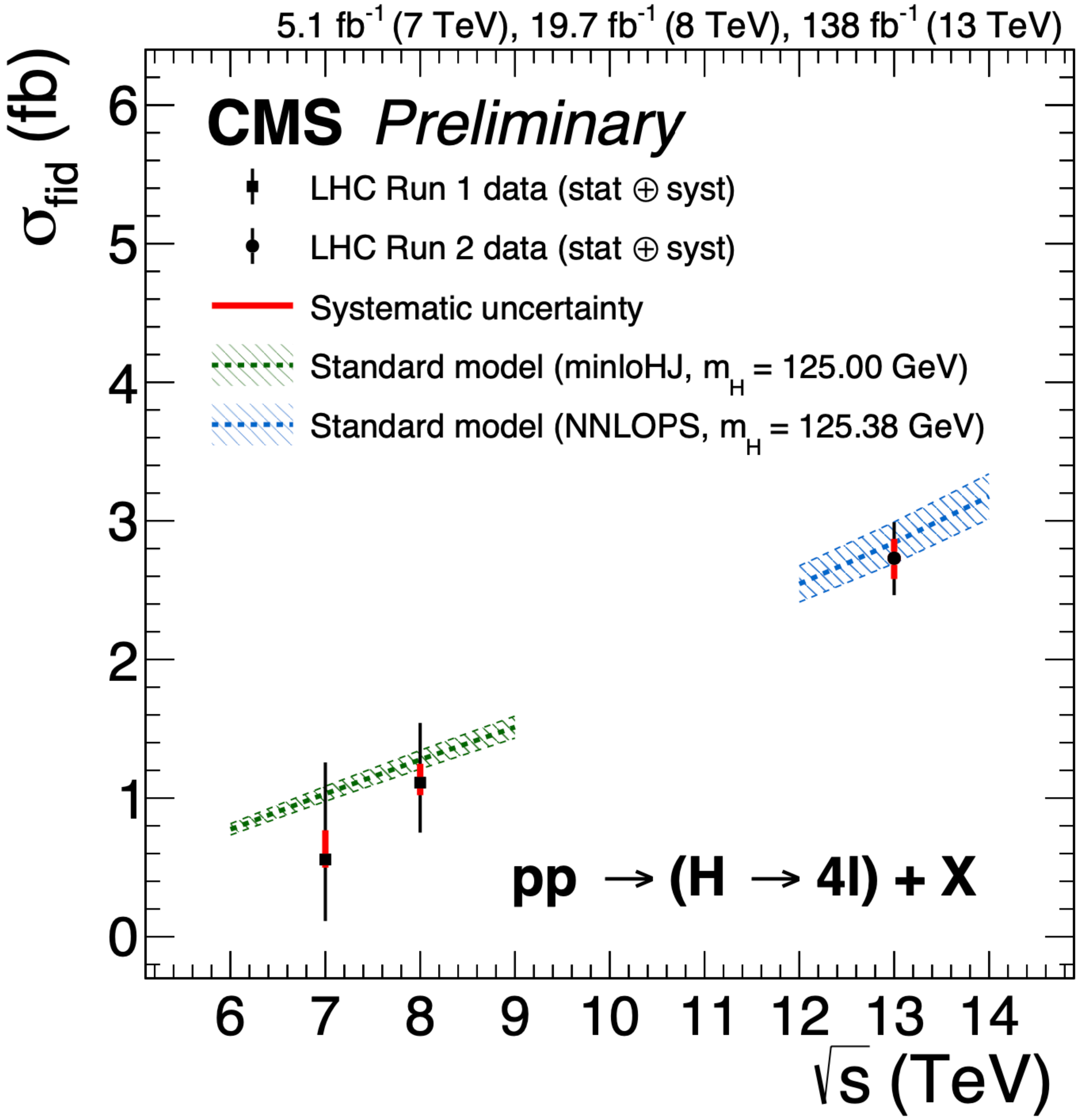

$$\sigma^{fid} = 2.73^{+0.22}_{-0.22}\,\text{(stat)}^{+0.15}_{-0.14}\,\text{(sys)} = 2.73^{+0.22}_{-0.22}\,\text{(stat)}^{+0.12}_{-0.12}\,\text{(ele)}^{+0.06}_{-0.05}\,\text{(lumi)}^{+0.04}_{-0.04}\,\text{(bkg)}^{+0.03}_{-0.03}\,\text{(muons)}$$

Inclusive cross section measurement comparison

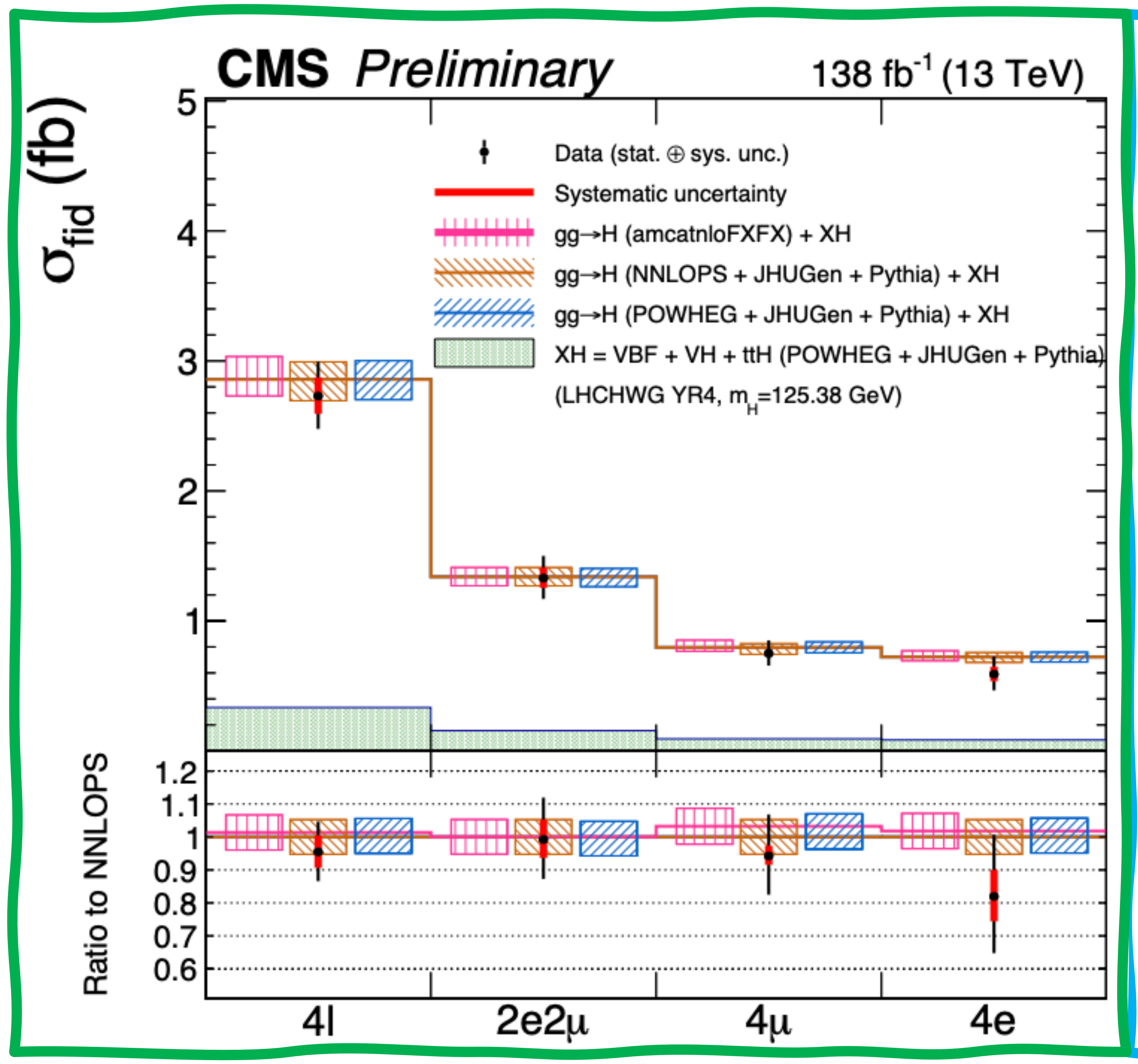

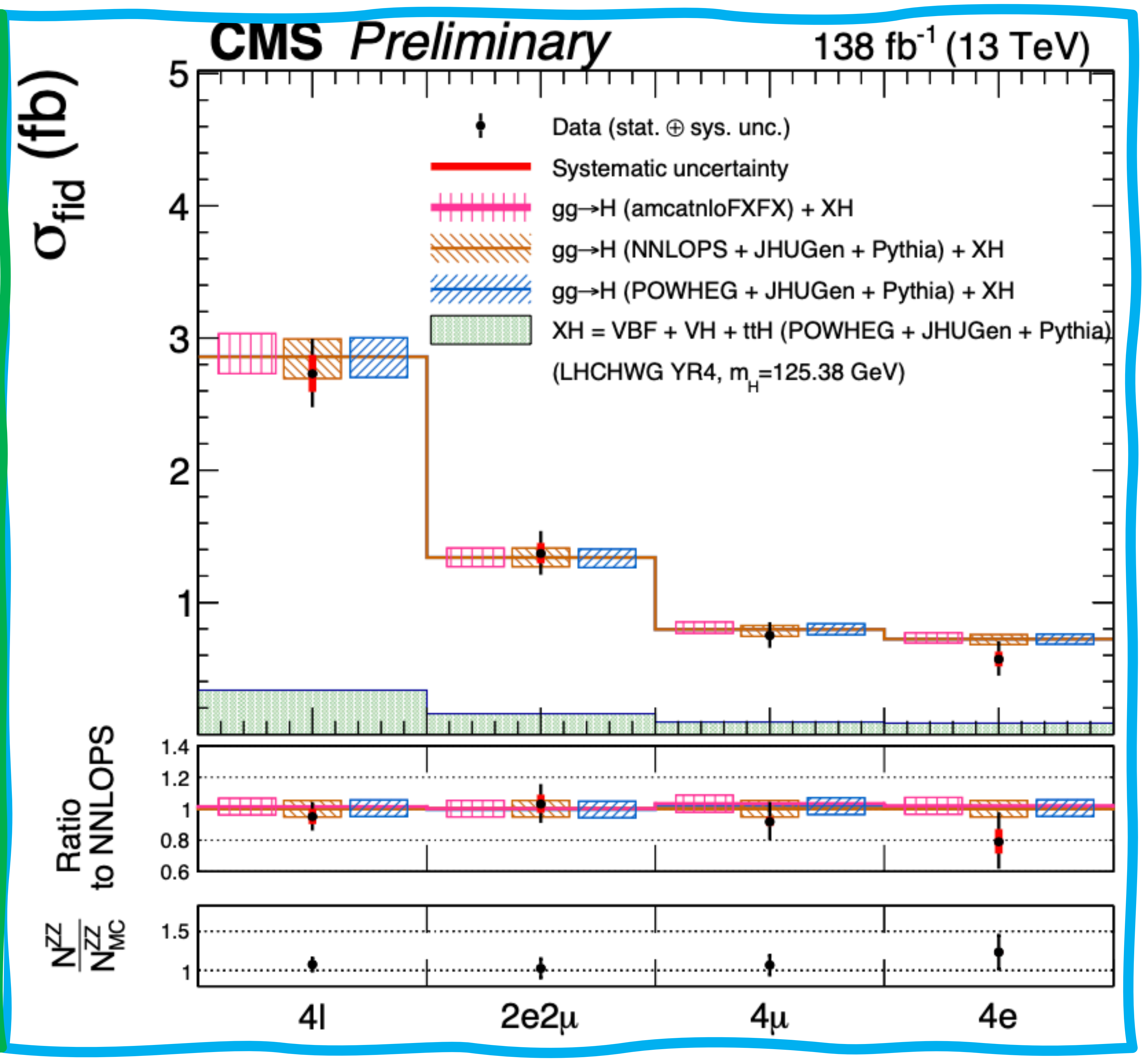

✳ Measured inclusive fiducial cross section of two methods

$$\sigma^{fid} = 2.73^{+0.22}_{-0.22}(stat)^{+0.15}_{-0.14}(sys)\,fb$$

$$\sigma^{fid} = 2.74^{+0.24}_{-0.23}(stat)^{+0.14}_{-0.11}(sys)\,fb$$

✳The measured inclusive fiducial cross section of

◉ (left) *Different final states* with the irreducible background normalization taken from MC simulation

◉ (right) *Different final states* with the irreducible backgrounds normalization ZZ floating in the fit

- Bottom panel shows ration between measured ZZ normalization and prediction from MC.

Inclusive fiducial cross section

Differential production observables

p_T^H $|y_H|$ p_T^{j1} N_{jets}

p_T^{Hj} m_{Hjj} p_T^{j2} T_B^{max} T_C^{max}

p_T^{Hjj} m_{jj} $|\Delta\eta_{jj}|$ $|\Delta\phi_{jj}|$

Differential decay observables

m_{Z1} m_{Z2} Φ Φ_1

$\cos(\theta_1)$ $\cos(\theta^*)$ $\cos(\theta_2)$

D_{0-}^{dec} D_{CP}^{dec} D_{0h+}^{dec} $D_{\Lambda1}^{dec}$ $D_{\Lambda1}^{Z\gamma,dec}$ D_{int}^{dec}

Double-differential observables

T_C^{max} vs p_T^H m_{Z1} vs m_{Z2}

N_{jet} vs p_T^H p_T^H vs p_T^{Hj}

$|y_H|$ vs p_T^H p_T^{j1} vs p_T^{j2}

Results: Differential

✴**Revised binning** w.r.t previous analyses

✴$p_T(H)$ spectrum measured with an average precision of **35%** (in some bins down to 20%)

✴**Extension of the jet phase space** (from $|\eta_{jet}| < 2.5$ to $|\eta_{jet}| < 4.7$); thanks to the improved CMS jet reconstruction

Results: Differential- Rapidity-weighted jet observables

Observables defined as the **transverse momentum of the jet weighed by a function of its rapidity.** They can be factorised and re-summed allowing for **precise theory predictions** and can be used as a test of **QCD resummation** since their resummation structure is different from p_T*(jet).*

$$\mathcal{T}_C^j = \frac{m_T^j}{2\cosh(y_j - Y_H)}$$

$$\mathcal{T}_B^j = m_T^j e^{-|y_j - Y_H|}$$

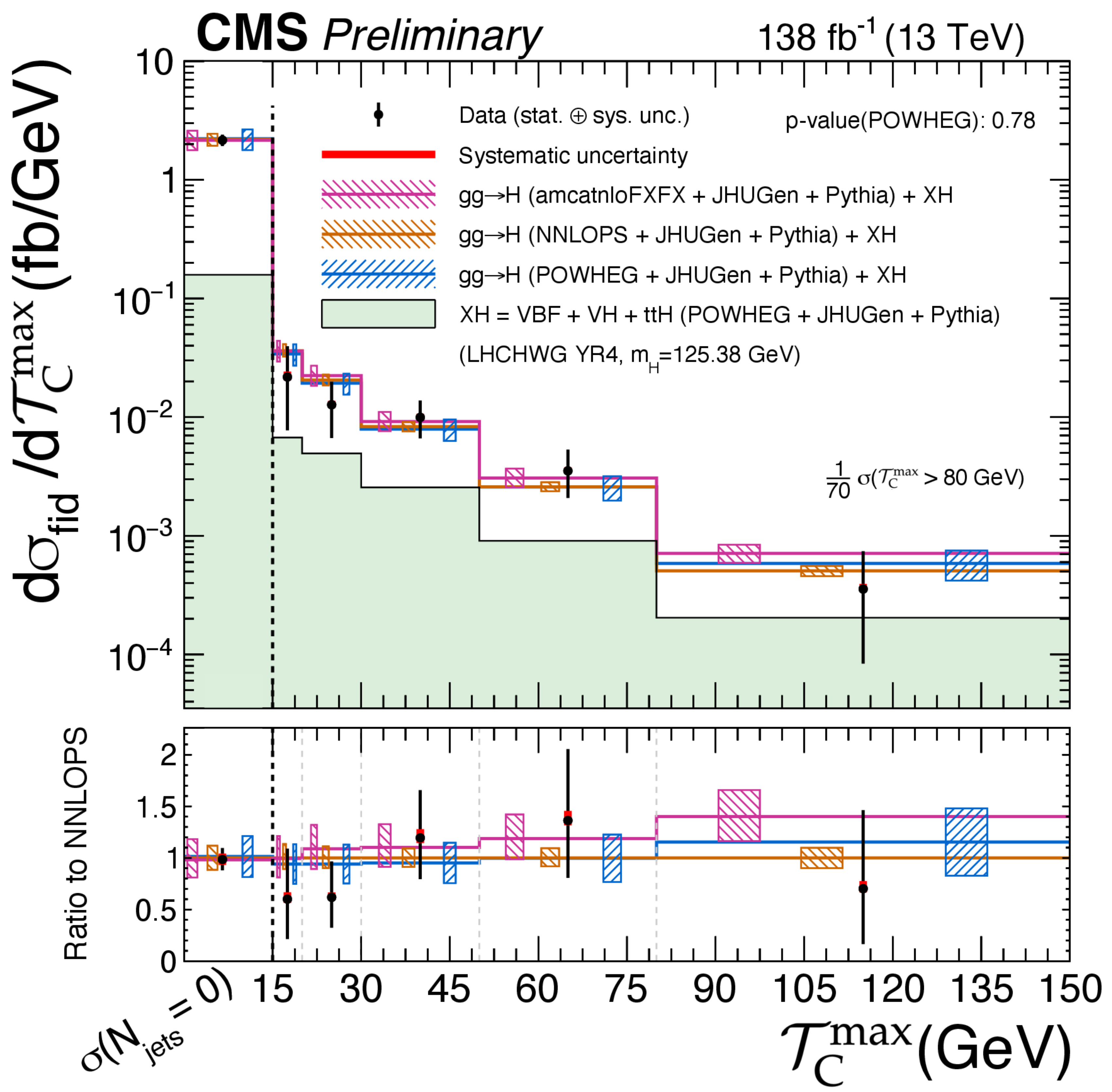

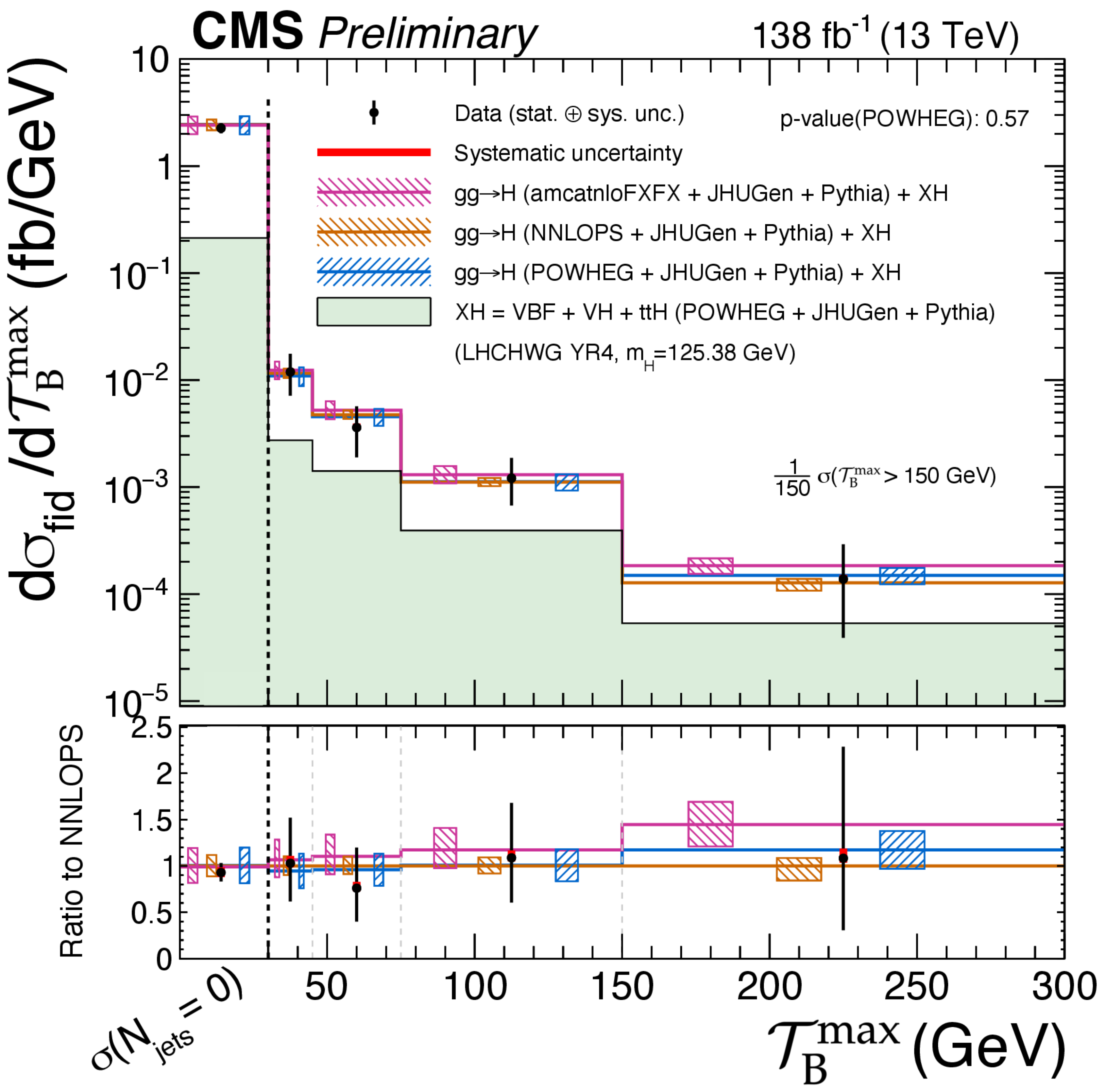

Results: Differential- Rapidity-weighted jet observables

Observables defined as the **transverse momentum of the jet weighed by a function of its rapidity.** They can be factorised and re-summed allowing for **precise theory predictions** and can be used as a test of **QCD resummation** since their resummation structure is different from *p_T(jet).*

$$\mathcal{T}_C^j = \frac{m_T^j}{2\cosh(y_j - Y_H)}$$

$$\mathcal{T}_B^j = m_T^j e^{-|y_j - Y_H|}$$

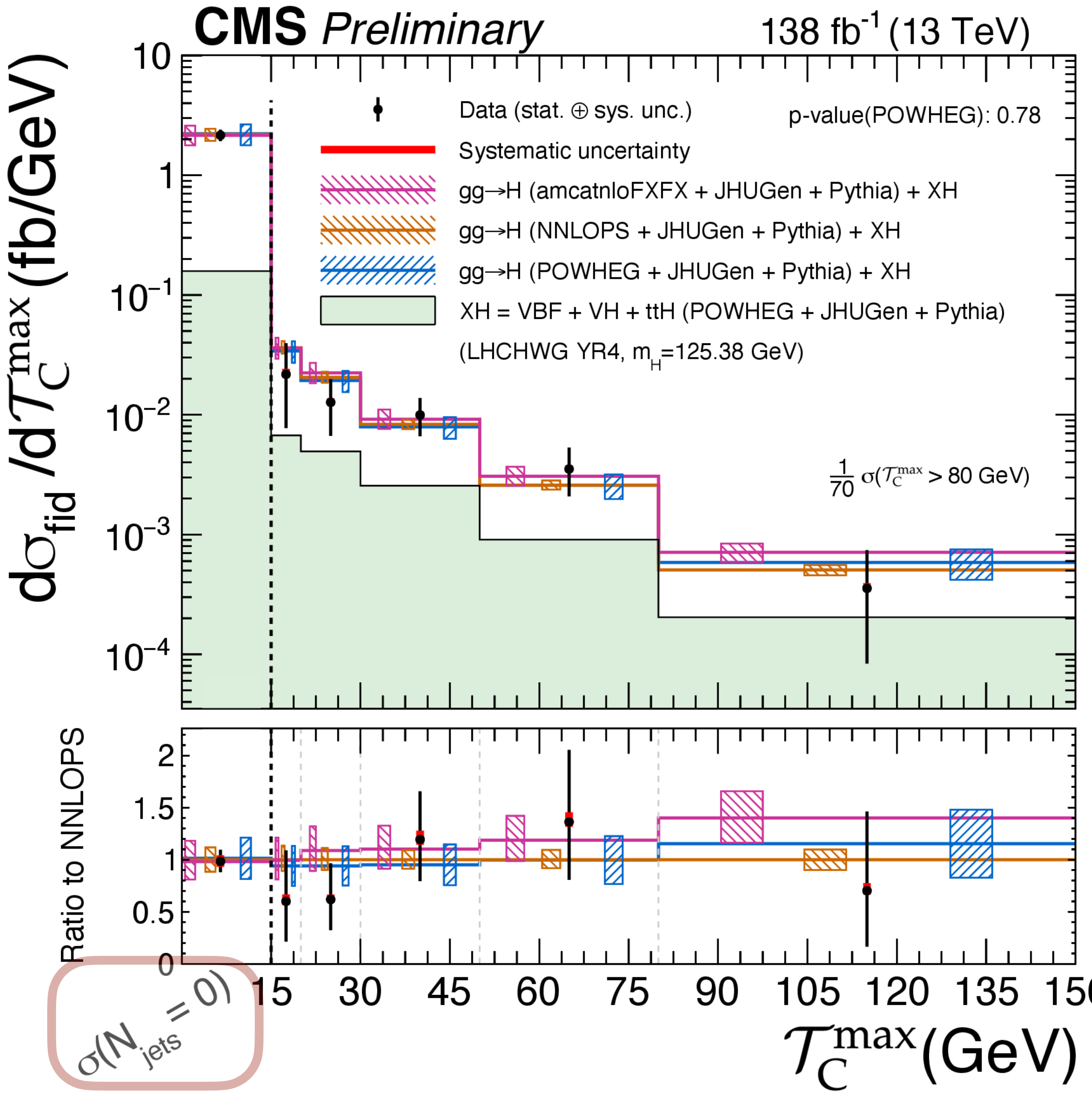

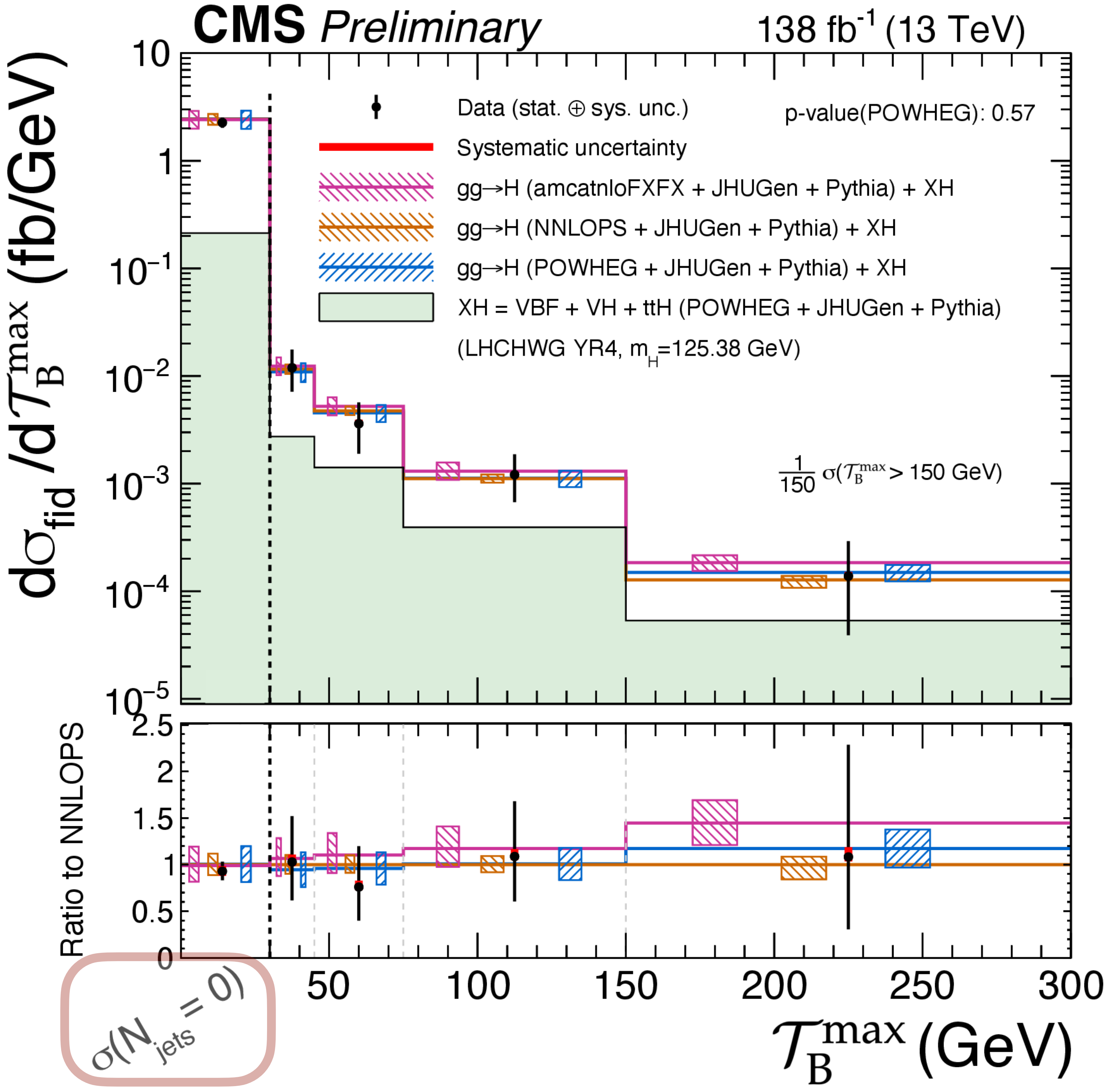

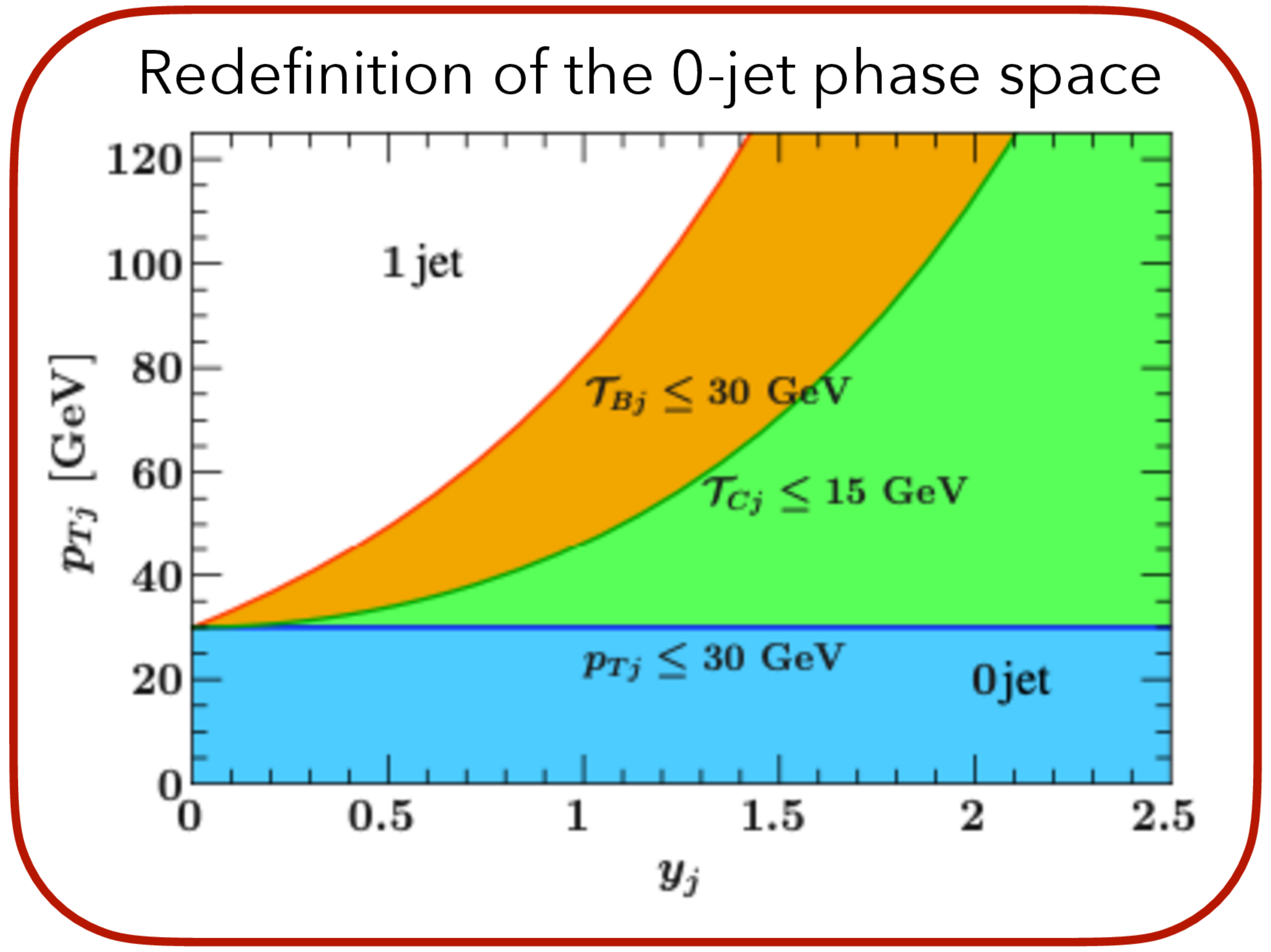

Phys.Rev.D 91 (2015) 5, 054023

Inclusive fiducial cross section

Differential production observables

p_T^H $|y_H|$ p_T^{j1} N_{jets}

p_T^{Hj} m_{Hjj} p_T^{j2} T_B^{max} T_C^{max}

p_T^{Hjj} m_{jj} $|\Delta\eta_{jj}|$ $|\Delta\phi_{jj}|$

Differential decay observables

m_{Z1} m_{Z2} Φ Φ_1

$\cos(\theta_1)$ $\cos(\theta^*)$ $\cos(\theta_2)$

D_{0-}^{dec} D_{CP}^{dec} D_{0h+}^{dec} $D_{\Lambda1}^{dec}$ $D_{\Lambda1}^{Z\gamma,dec}$ D_{int}^{dec}

Double-differential observables

T_C^{max} vs p_T^H m_{Z1} vs m_{Z2}

N_{jet} vs p_T^H p_T^H vs p_T^{Hj}

$|y_H|$ vs p_T^H p_T^{j1} vs p_T^{j2}

Interpretations

k_λ, k_c, k_b

Results: Differential- Decay observables

The kinematics of the decay of the H boson in 4 leptons is fully described by the Higgs boson's mass and 7 parameters:

- ✳ The two **Z masses** (**Z1** and **Z2**)
- ✳ **Three angles** describing the **fermion kinematics** (Φ, $\cos\theta_2$, $\cos\theta_1$)
- ✳ **Two angles** connecting **production to decay** (Φ_1, $\cos\theta^*$)

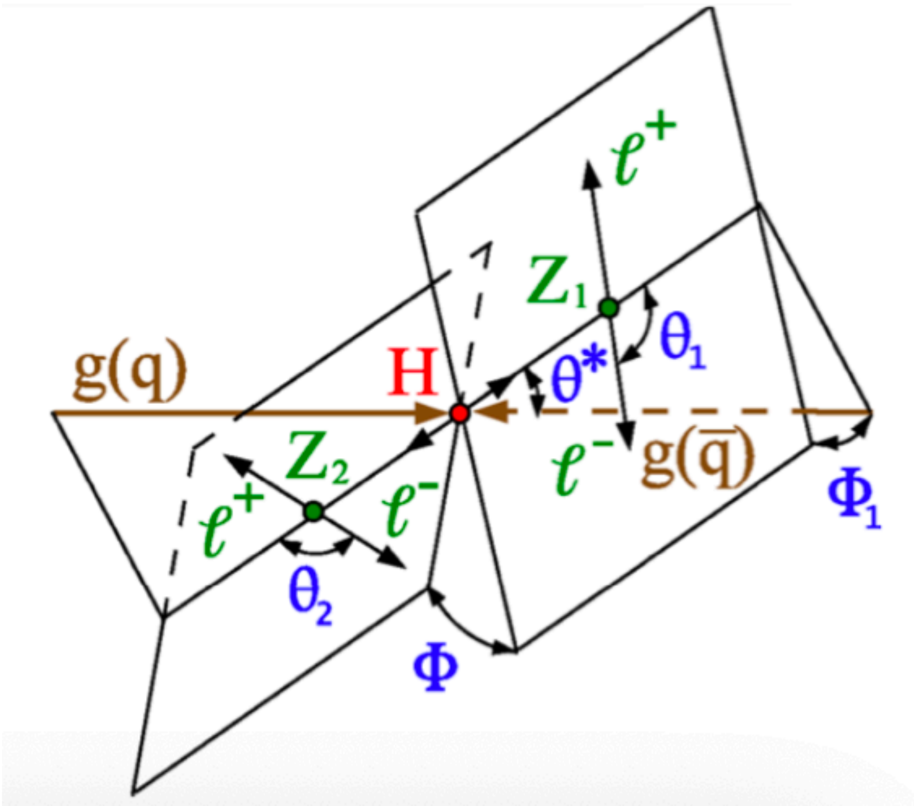

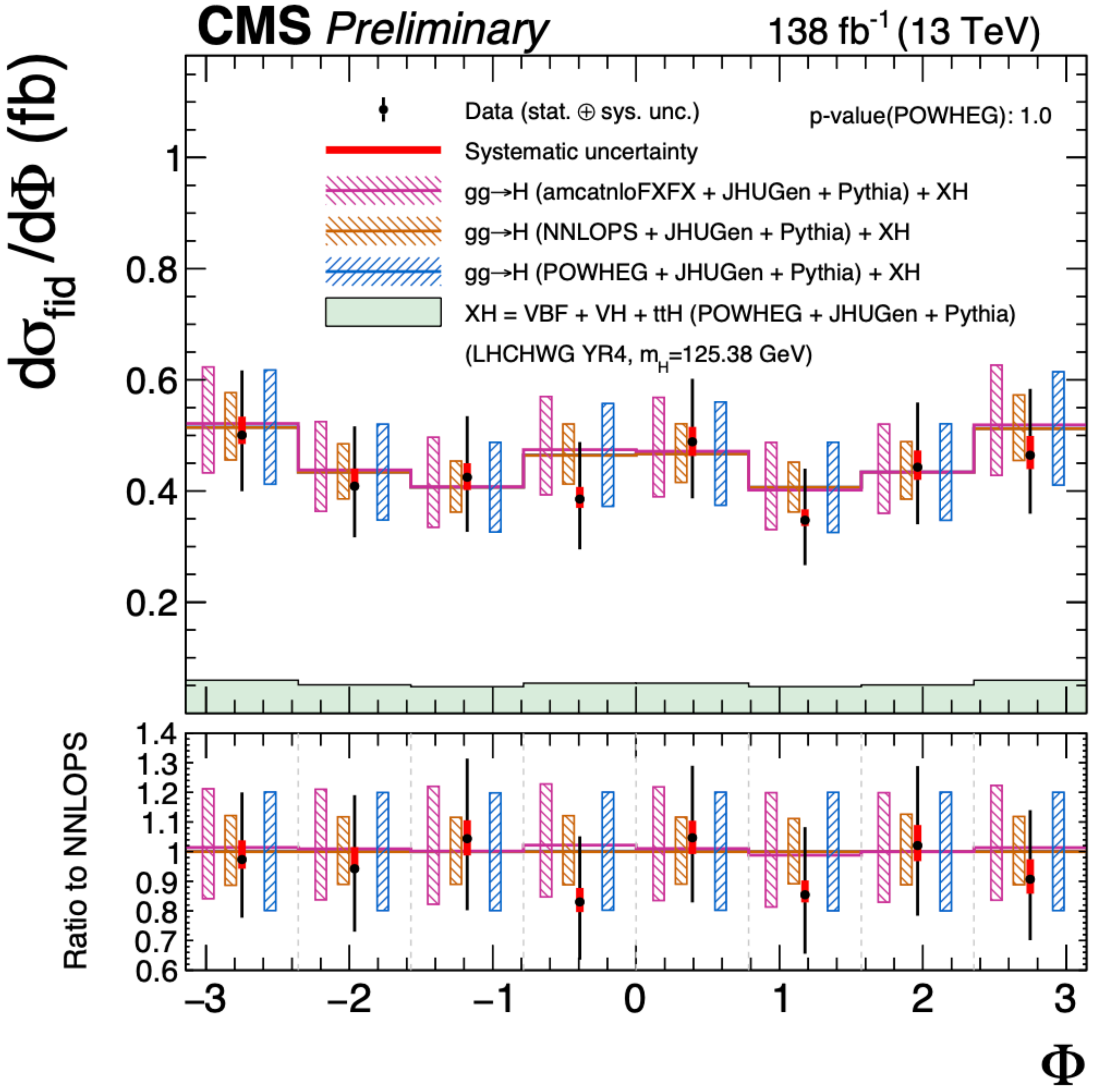

Results for decay observables are presented in **2e2mu** and **4e+4mu** final states as well.

The **same-flavour lepton interference** makes the shapes in 2e2mu and 4e/4mu final states different

Results: Differential- Decay observables

The kinematics of the decay of the H boson in 4 leptons is fully described by the Higgs boson's mass and 7 parameters:

- ✳ The two **Z masses** (**Z1** and **Z2**)
- ✳ **Three angles** describing the **fermion kinematics** (Φ, $\cos\theta_2$, $\cos\theta_1$)
- ✳ **Two angles** connecting **production to decay** (Φ_1, $\cos\theta^*$)

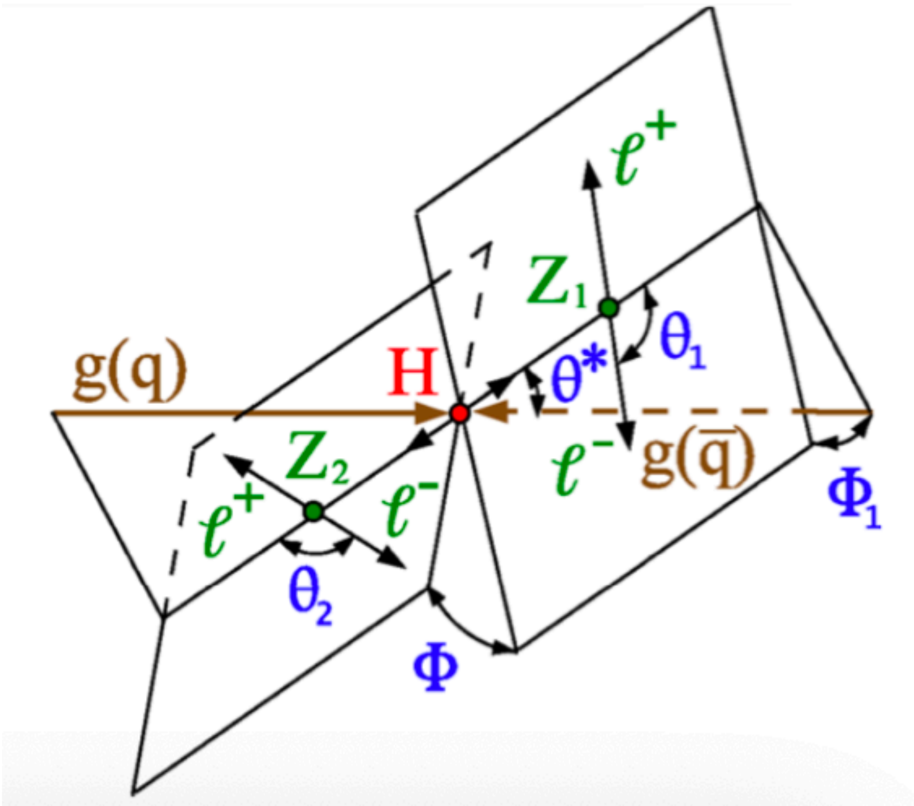

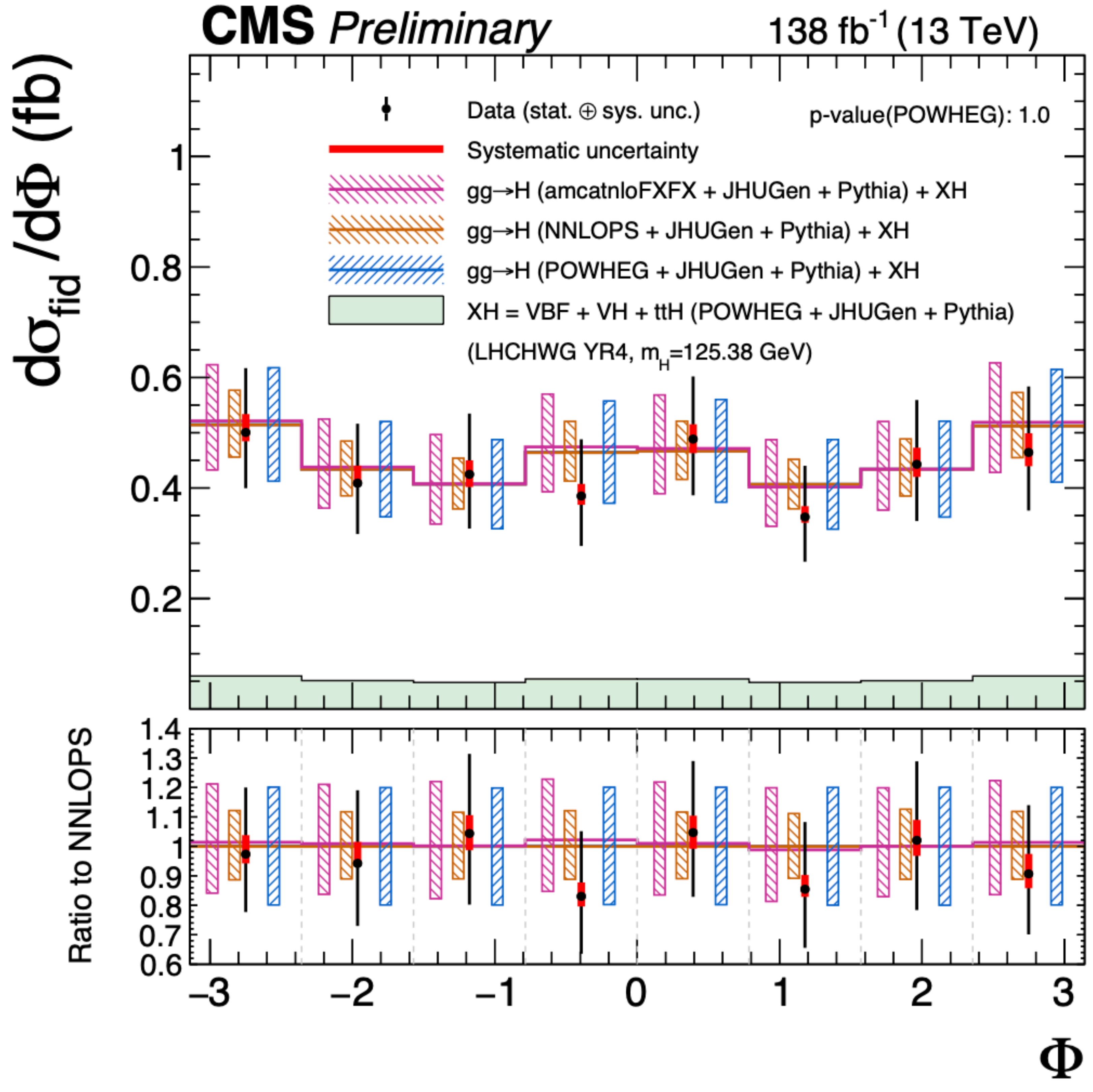

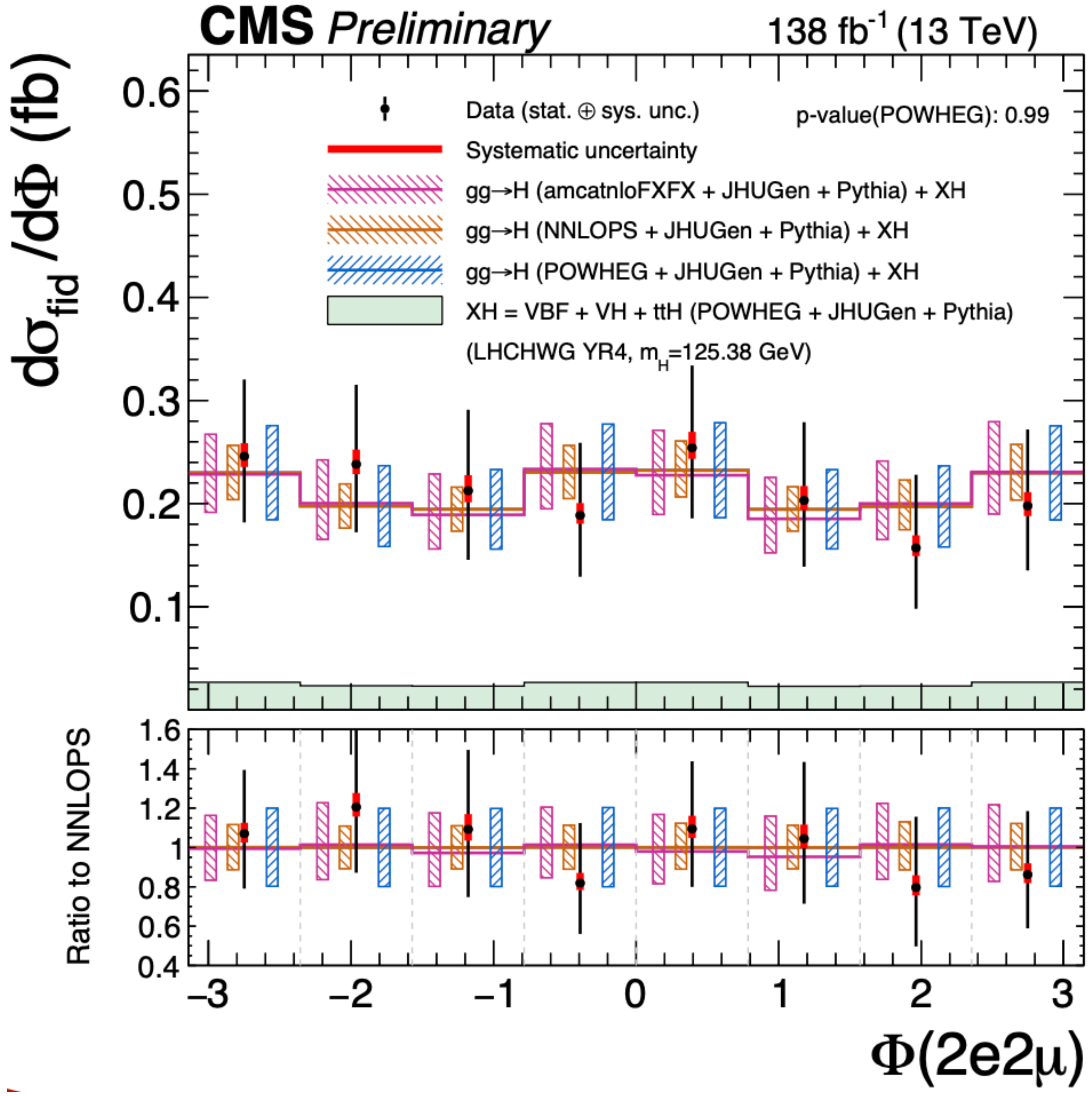

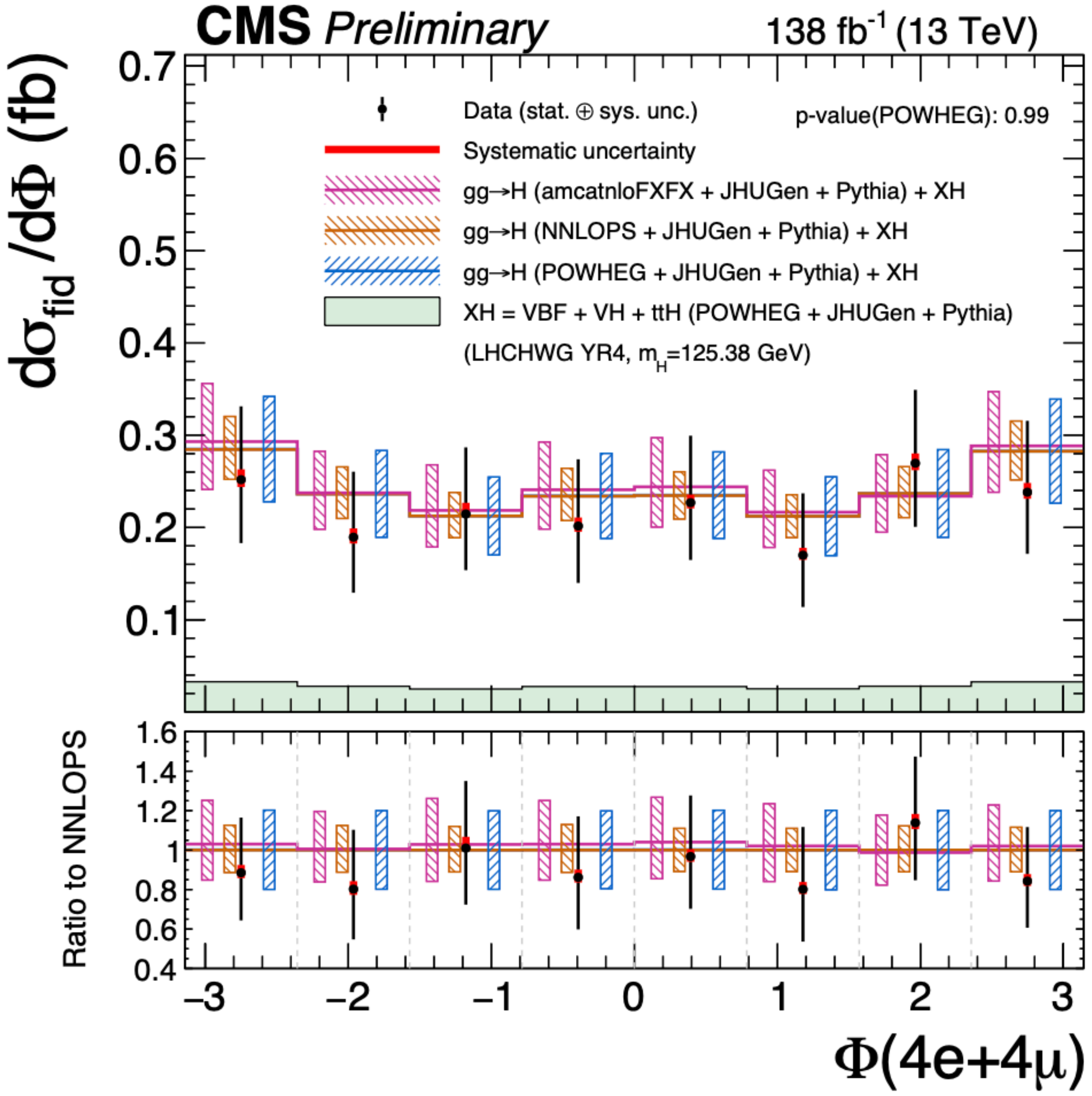

Results: Differential- Matrix Elements Discriminants

Probe **HZZ vertex** via **Matrix-Element discriminants** sensitive to BSM physics

$$A(HV_1V_2)=\frac{1}{v}\left\{ M_{V_1}^2\left(g_1^{VV}+\frac{\kappa_1^{VV}q_1^2+\kappa_2^{VV}q_2^2}{\left(\Lambda_1^{VV}\right)^2}+\frac{\kappa_3^{VV}(q_1+q_2)^2}{\left(\Lambda_Q^{VV}\right)^2}+\frac{2q_1\cdot q_2}{M_{V_1}^2}g_2^{VV}\right)(\varepsilon_1\cdot\varepsilon_2) -2g_2^{VV}(\varepsilon_1\cdot q_2)(\varepsilon_2\cdot q_1)-2g_4^{VV}\varepsilon_{\varepsilon_1\varepsilon_2 q_1 q_2}\right\}$$

Tree-level SM
$g_1^{ZZ} = g_1^{WW} = 2$

Coupling	g_4^{ZZ}	g_2^{ZZ}	k_1^{ZZ}	$k_2^{Z\gamma}$
Discriminants to separate hypothesis	$\mathscr{D}_{0-}^{dec}$	$\mathscr{D}_{0h+}^{dec}$	$\mathscr{D}_{\Lambda 1}^{dec}$	$\mathscr{D}_{\Lambda 1}^{Z\gamma,dec}$
Interference discriminants	$\mathscr{D}_{CP}^{dec}$	$\mathscr{D}_{int}^{dec}$	-	-

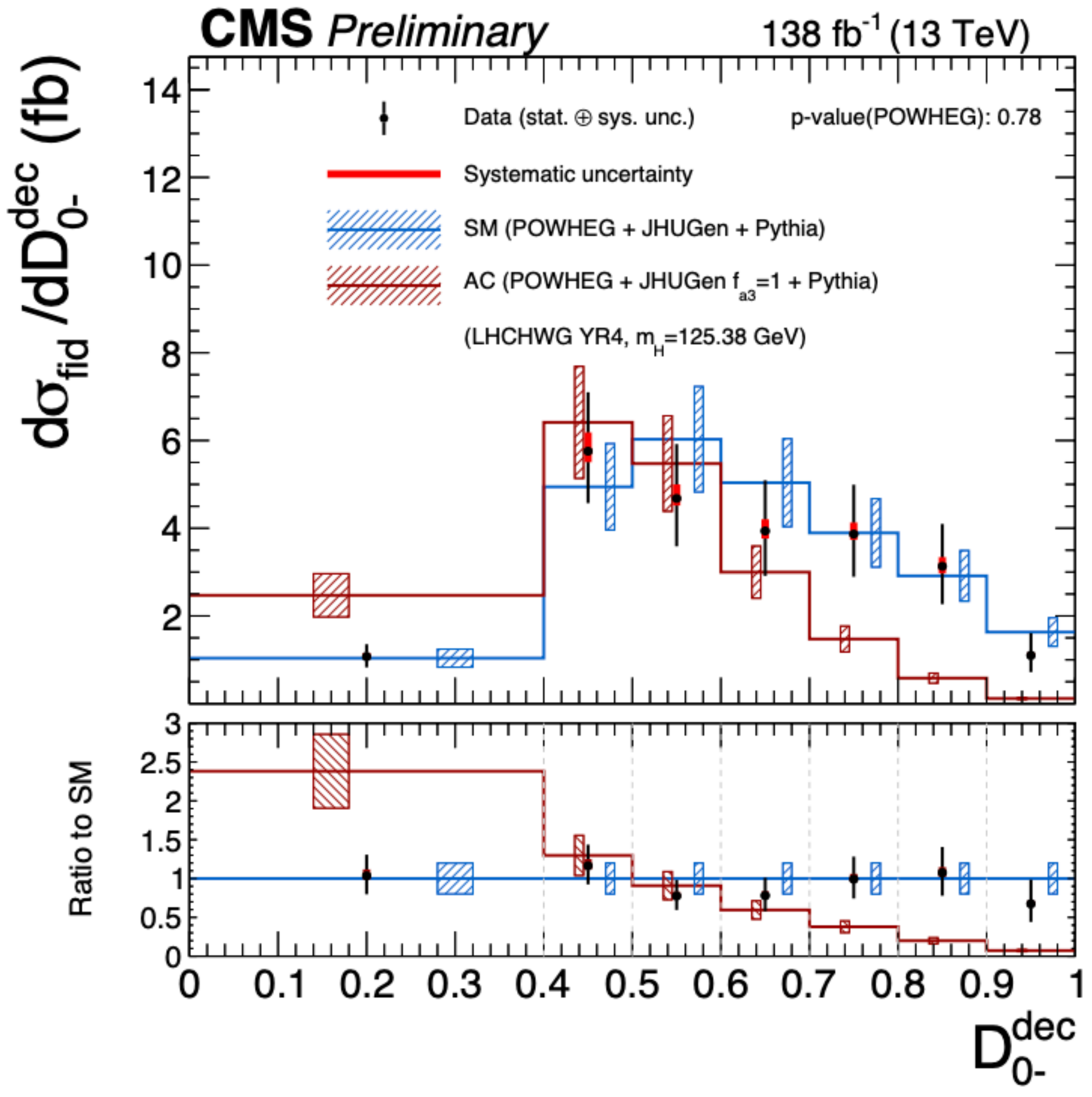

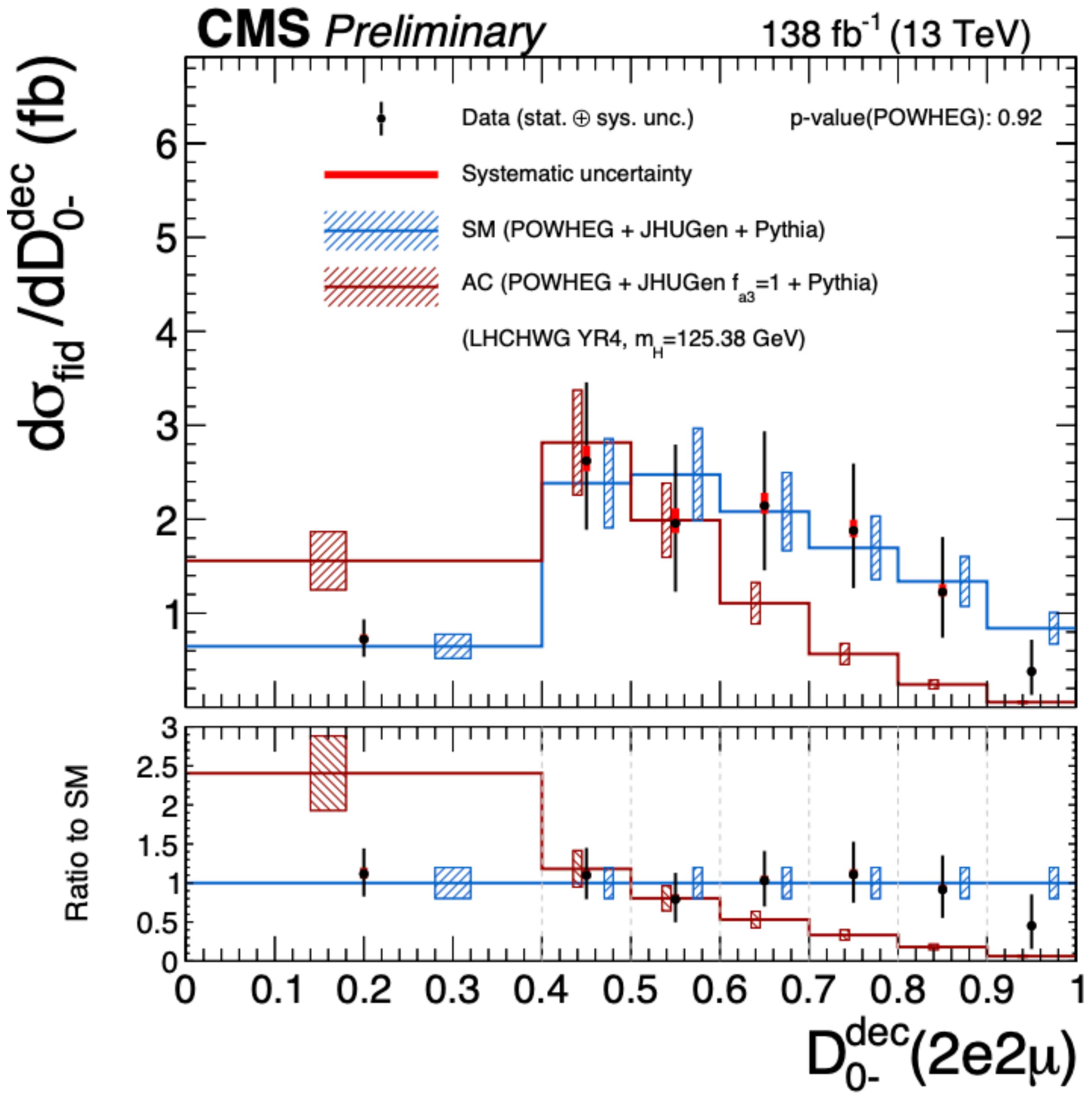

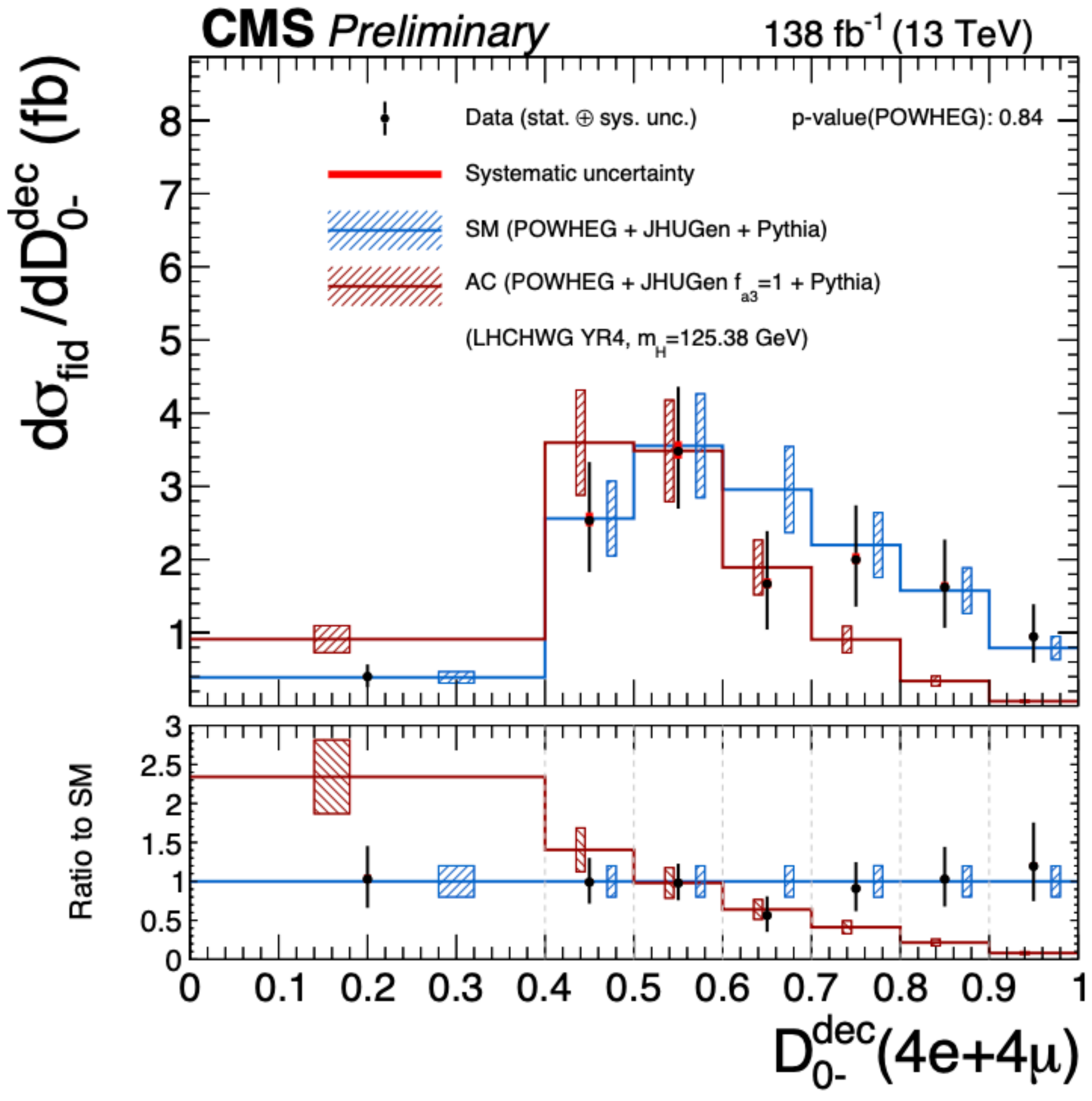

Inclusive fiducial cross section

Differential production observables

p_T^H $|y_H|$ p_T^{j1} N_{jets}

p_T^{Hj} m_{Hjj} p_T^{j2} T_B^{max} T_C^{max}

p_T^{Hjj} m_{jj} $|\Delta\eta_{jj}|$ $|\Delta\phi_{jj}|$

Differential decay observables

m_{Z1} m_{Z2} Φ Φ_1

$\cos(\theta_1)$ $\cos(\theta^*)$ $\cos(\theta_2)$

D_{0-}^{dec} D_{CP}^{dec} D_{0h+}^{dec} $D_{\Lambda1}^{dec}$ $D_{\Lambda1}^{Z\gamma,dec}$ D_{int}^{dec}

Double-differential observables

T_C^{max} vs p_T^H

m_{Z1} vs m_{Z2}

N_{jet} vs p_T^H

p_T^H vs p_T^{Hj}

$|y_H|$ vs p_T^H

p_T^{j1} vs p_T^{j2}

Results: Differential- Decay observables

An extensive set of **double** differential observables to probe specific phase space regions

(i) τ_C^{max} vs p_T^H (ii) m_{Z1} vs m_{Z2} (iii) N_{jet} vs p_T^H (iv) p_T^H vs p_T^{Hj} (v) $|y_H|$ vs p_T^H (vi) $\mathbf{p_T^{j1}}$ **vs** $\mathbf{p_T^{j2}}$